Alma Mater Studiorum – Università di Bologna

DOTTORATO DI RICERCA IN

Biologia cellulare e molecolare

Ciclo XXXV

Settore Concorsuale: 05/E2

Settore Scientifico Disciplinare: BIO/11

Characterisation of RNase Y in *H. pylori*: a non-essential enzyme involved in the processing of *cag*-PAI non coding RNA 1 (CncR1) sRNA

Presentata da: Federico D'Agostino

Coordinatore Dottorato

Prof. Vincenzo Scarlato

Supervisore

Prof. Vincenzo Scarlato

Co-supervisore

Prof. Davide Roncarati

Esame finale anno 2023

Abstract

The importance of *Helicobacter pylori* as a human pathogen is underlined by the plethora of diseases it is responsible for. This bacterium colonizes the human gastro-intestinal tract (i.e., the only known reservoir) of almost half of the world's population and its infections commonly persist throughout life. The capacity of *H. pylori* to adapt to the restricted host-associated environment and to evade the host immune response largely depends on its streamlined and efficient signalling network. The peculiar *H. pylori* small genome size combined with its paucity of transcriptional regulators highlights the relevance of post-transcriptional regulatory mechanisms as small non-coding RNAs (sRNAs). However, among the 8 RNases represented in *H. pylori* genome, a regulator guiding sRNAs metabolism is still not well studied.

In the presented Ph.D. project, we investigated for the first time the physiological role in *H. pylori* G27 strain of the RNase Y enzyme. Further, we characterized a previously unreported activity on *cag*-PAI non coding RNA 1 (CncR1) sRNA.

To pursue these goals, we followed three major research lines. In the first one we provide a comprehensive characterization of the RNase Y activity by analysing its genomic organization and the factors that orchestrate its expression. Then, based on bioinformatic prediction models, we depict the most relevant determinants of RNase Y function, demonstrating a correlation of both structure and domain organization with orthologues represented in Gram-positive bacteria. To unveil the post-transcriptional regulatory effect exerted by the RNase Y, we compared the transcriptome of an RNase Y knock-out mutant to the parental wild type strain by RNA-seq approach.

In the second line of research we characterized the activity of this single strand specific endoribonuclease on CncR1. We found that deletion or inactivation of RNase Y led to the accumulation of a 3'-extended CncR1 (CncR1-L) transcript over time. Moreover, beneath its increased half-life, CncR1-L resembled a CncR1 inactive phenotype.

Finally, we focused on the characterization of the in vivo interactome of CncR1. We set up a preliminary MS2-affinity purification coupled with RNA-sequencing (MAPS) approach and we evaluated the enrichment of specific targets, demonstrating the suitability of the technique in the *H. pylori* G27 strain.

Content

1. Introduction

1.1 *Helicobacter pylori*

Helicobacter pylori is a microaerophilic, spiral-shaped, Gram-negative pathogen belonging to the phylum of *Campylobacterota* (formerly termed ε-proteobacteria) (Waite *et al.*, 2017). Its only known natural reservoir is the human stomach, where it can commonly persist throughout life if not treated. Although *H. pylori* infections generally have an asymptomatic outcome, since its isolation in 1982 its presence in the gastric niche has been related to many gastrointestinal disorders such as chronic active gastritis (Marshall and Warren, 1984), gastric and duodenal ulcer diseases (Nomura *et al.,* 1994), mucosa-associated lymphoid tissue (MALT) lymphoma and gastric adenocarcinoma (Vogelmann and Amieva, 2007; Du and Isaccson, 2002).

The exact route of *H. pylori* transmission is poorly understood. Evidences support that the bacterium is usually acquired during childhood in the household environment as a consequence of an oral-oral (i.e. saliva) or faecal-oral (i.e. contaminated food) transmission route. Indeed, factors like poor hygiene conditions and overcrowding are thought to promote a horizontal transmission of the pathogen (Kayali *et al.,* 2018). The establishment of long-term *H. pylori* colonization relies on the concerted expression of several virulence factors associated with acid acclimation, cell motility, adherence and gastric epithelial cell pathogenicity. The details of these complex mechanisms are exhaustively described in the literature (Ansari, Yamaoaka, 2007; Ansari and Yamaoaka, 2019). Upon entering the gastric micro-environment, the massive production of urease accounts for the neutralization of the strong acidic pH of around 2 and the maintenance of the periplasmic pH close to 6.1, thus providing the necessary conditions for *H. pylori* survival. The number of flagella and the flagellar-mediated motility, further aided by the bacterial helical shape, allow the bacterium to move in a corkscrew-like fashion from the gastric lumen, penetrate the mucous layer and colonize the gastric epithelium. Then, the wide range of adhesins displayed at the *H. pylori* outer membrane provides bacterial attachment to the host epithelium. Finally, the production of multiple fundamental pathogenicity factors leads to host immune response modulation and the onset of *H. pylori*-dependent gastric disease. Among these, the extracellular translocation of the CagA cytotoxin mediated by the type IV secretion system (T4SS) and the production of the pore-forming toxin VacA mainly hamper the epithelial tissue integrity by disrupting cell polarity and stimulating the host inflammatory response (i.e., pro-inflammatory cytokines production).

Although *H. pylori* prevalence has declined in most industrialized countries in the last decades, it is still considered a major global public health issue. In 2015 more than 50% of the world population was estimated to be infected with *H. pylori*, with a higher prevalence in Africa (79.1%), Latin America (63.4%), and Asia (54.7%) (Hooi *et al.*, 2017).

Until the early 2000s, the recommended *H. pylori* eradication treatment consisted of a 7-day triple therapy with a proton pump inhibitor, amoxicillin and clarithromycin (Malfertheiner *et al.*, 2007). However, the increasing outbreak of clarithromycin- and multiple-resistant phenotypes led to a significant reduction in the eradication rate achieved with this regimen. Recently, international guidelines recommended using 10-14 days of bismuth- or non-bismuth-based quadruple therapies containing a proton pump inhibitor and two or three antibiotics, including amoxicillin, clarithromycin, metronidazole, nitroimidazole and tetracycline (Malfertheiner *et al.*, 2017; Suzuki *et al.*, 2019).

In 1994 *H. pylori* was classified by the World Health Organization (WHO) as a group I carcinogen. In 2017 the same WHO included clarithromycin-resistant *H. pylori* in its first-ever published list of antimicrobial resistant priority pathogens posing the greatest threat to human health.

1.2 Genome and regulatory functions

In 1997, Tomb and co-workers published the first complete genome sequence of *H. pylori* 26695 (Tomb *et al.*, 1997). Since then, the sequences of many other strains, including J99, G27 and N6, have been annotated, revealing a remarkably similar genomic organization, gene order and predicted gene products (Baltrus *et al.*, 2009; Behrens *et al.*, 2012). *H. pylori* shows a small AT-rich (>60%) genome of about ~1.63 Mb in size, coding for a median of 1440 proteins.

H. pylori is an emblematic example of how the specialist lifestyle due to a restricted ecological niche (i.e., gastrointestinal tract) led to the evolution of a streamlined and efficient signalling network (Mo *et al.*, 2022). As a result, *H. pylori* transcriptional machinery revealed a low complexity and redundancy degree (Alm *et al.*, 1999; Scarlato *et al.*, 2001; Vannini *et al.*, 2022). As a comparison, the RNA polymerase (RNAP) core enzyme of the Gram-negative archetype *E. coli* is composed of 5 subunits ($\alpha_2\beta\beta'\omega$) and 1 sigma ($\sigma$) factor. In contrast, in *H. pylori*, the *rpoB* and *rpoC* genes, which encode for the β and β' subunits of the RNAP catalytic core, are fused into a unique polypeptide. Moreover, *H. pylori* possesses only three sigma factors: the vegetative σ^{80} (RpoD) controlling the transcription of most genes, and two alternative sigma factors, σ^{54} (RpoN) and σ^{28} (FliA), involved in the programmed expression of class II and class III flagellar genes, respectively (Niehus *et al.*, 2004). The consensus

sequence for the σ^{80} factor in *H. pylori* promoters shows a peculiar organization. Indeed, the almost ubiquitously conserved regulatory -35 (TTGACA) element is replaced by a periodic AT-rich stretch upstream of position -14 from the transcriptional start site (TSS), followed by an extended -10 Pribnow box (tgnTAtaAT) (Sharma *et al.,* 2010).

Besides the three σ factors, *H. pylori* codes for a small number of 14 dedicated transcriptional regulators. Among these, four complete two-component systems control the transcription of genes mainly involved in chemotaxis and flagellar biogenesis (CheY1Y2A and FlgRS), acid acclimation (ArsRS) and copper homeostasis (CrdRS) (Brahmachary *et al.,* 2004; Foynes *et al.,* 2000; Loh *et al.,* 2021; Waidner *et al.,* 2005). Then, two orphan response regulators coordinate chromosome replication and acetone metabolism (HP1021) and act as a master regulator of crucial cellular processes (HP1043) (Donczew *et al.,* 2015; Pelliciari *et al.,* 2017; Zannoni *et al.,* 2021). Finally, among the other transcriptional regulators, four are involved in stress response (HspR and HrcA) and metal ions homeostasis (Fur and NikR), while the other four have putative, not well-characterized functions (HP1139, HP0222, HP0564 and HP0835) (Breswill *et al.,* 1998; Contreras *et al.,* 2003; Roncarati and Scarlato, 2018; Vannini *et al*., 2022).

Regardless of the scarcity of transcriptional regulators, in the last few years a fundamental role in the control of gene expression and adaptation to the hostile environment has been attributed to post-transcriptional regulatory mechanisms. The primary transcriptome analysis of the *H. pylori* 26695 strain revealed a vast antisense transcription (>900 antisense RNAs) that is uncorrelated with the local GC content and evidenced the expression of hundreds of small RNAs (sRNAs), of which more than 60 have been validated (Sharma *et al.,* 2010). In addition, *H. pylori* retains most of the widely conserved prokaryotic riboregulators, such as the 6S RNA, the ribozyme RNase P and the transfer messenger RNA (tmRNA). Interestingly, riboswitches are almost not represented, and only one riboswitch is predicted upstream of the *pnuC* gene (Sharma *et al.,* 2010).

Therefore, compared to other pathogens, *H. pylori* presumably builds its ability to adapt to a constantly changing environment on different mechanisms in addition to transcriptional regulation.

1.3 Non-coding RNAs (ncRNAs) mediated post-transcriptional regulation

1.3.1 *Cis*-encoded antisense RNAs (asRNAs)

Cis-encoded antisense RNAs (asRNAs) are RNA regulatory elements transcribed from the complementary strand of their target genes. They can be generated from 5'- or 3'-untranslated regions (UTRs), thus ranging from a few hundred nucleotides in size, or encompassing all the target sequence up to a few thousand nucleotides. Due to the almost perfect complementarity, asRNAs form extensive RNA::RNA duplexes and influence the stability of the target RNA with different outcomes (Thomason *et al.,* 2010; Georg *et al.,* 2011). Post transcriptional regulation based on asRNAs is thought to be highly represented in *H. pylori*, as at least one antisense TSS is associated with 46% of all ORFs. Some of such regulatory modules have been characterised and found to be involved in crucial gene processes related to cell growth, virulence and rRNA maturation.

IsoA1-6 is a family of structurally related ~80 nt asRNAs transcribed from the opposite strand of small ORFs of homologous peptides named AapA1-6. The *aapA1-isoA1* locus represents the first ever described type I toxin-antitoxin system in *H. pylori* (Sharma *et al.,* 2010; Arnion *et al.,* 2017). The AapA1 toxin is a 30 aa-long hydrophobic peptide that, upon expression, targets the inner membrane and triggers a morphological transition from the typical helical shape to round coccoid cells. AapA1 toxin shows a multi-layered control of expression, including the interaction of its mature transcript with *isoA1* antitoxin followed by RNase III-driven degradation. Under stress conditions (i.e., oxidative stress), the activity of *isoA1* promoter is reduced. Hence AapA1 is actively translated, thus allowing the morphological transition. The coccoid state has been associated with a dormant phase of the cells that could be responsible for the refractoriness of the therapy regimen (El Mortaji *et al.,* 2020).

Another well-characterised mechanism of cis-encoded asRNA-mediated regulation involves the acid acclimation process. In *H. pylori*, the *ureAB* operon is responsible for the production of the UreA and UreB subunits of the urease enzyme. Under acidic conditions, the phosphorylated ArsR response regulator binds the *ureAB* promoter and ensures increased urease production. However, at neutral pH the unphosphorylated ArsR induces the expression of a 290 nt long 5'*ureB*-asRNA from the complementary *ureB* strand. Following the interaction with the 5' region of *ureB* along its entire sequence, 5'*ureB*-asRNA cause a premature transcription termination of the *ureAB* operon, leading to diminished urease production (Wen *et al.,* 2011).

A conserved and highly expressed asRNA was further identified at the 23S-5S rRNA locus (Sharma *et al.,* 2010). This asRNA interacts with the 5' leader region of the 23S-5S precursor

to form an intermolecular duplex cleaved by RNase III. This initial processing step induces additional cleavages in the rRNA precursor that will lead to mature 23S and 5S molecules and the degradation of the asRNA (Iost *et al.,* 2019).

1.3.2 *Trans*-encoded small RNAs (sRNAs)

Trans-encoded small RNAs (sRNAs) are a heterogeneous group of short (from ~50 nt to ~500 nt) structured RNA elements that exert a regulatory activity on mRNA targets encoded on a different locus. Differently from asRNAs, sRNAs transcripts fold into complex secondary structures and interact with a multiplicity of mRNA targets through partial or complete complementarity of a short (<20 nt) seed sequence. sRNAs biogenesis generally starts from a promoter located in the intergenic regions (IGRs) or overlaps ORFs (i.e. 5'UTR- and 3'UTR-derived sRNAs). Nevertheless, increasing clues support the formation of sRNAs following the processing of a precursor mRNA (Chao and Vogel., 2016) or tRNA (Lalaouna *et al.,* 2015). sRNAs can act through several different mechanisms to upregulate or downregulate their targets. Target gene downregulation mainly occurs when an sRNA binds to the 5' UTR of the mRNA target close to the ribosome binding site (RBS), thus preventing the ribosome assembly and the translation initiation. In most cases, this interaction leads to the cleavage of the mRNA target due to an endoribonuclease as RNase E or RNase Y in Gram-negative or Gram-positive bacteria, respectively. Nevertheless, non-canonical regulation pathways have been documented to date. The interaction between the sRNA regulator and its target can lead to the disruption of inhibitory secondary structures close to the ribosome binding site (RBS), thus favouring ribosome access to the Shine-Dalgarno (SD) and translation initiation (Carrier *et al.,* 2018; Prevost *et al.,* 2007).

Protein factors are frequently involved in the trans-acting sRNA-mediated regulation. Hfq is a homoexameric RNA chaperone belonging to the Sm/Lsm family that promotes the formation and the stabilisation of the sRNA:mRNA complexes in many bacteria (Vogel and Luisi, 2011). Conversely, in *Salmonella typhimurium*, the RNA chaperone ProQ was shown to promote RaiZ sRNA stabilisation but not to mediate its pairing with target mRNA (Smirnov *et al.,* 2016).

As 50% of all bacteria, *H. pylori* lacks homologues of both the RNA chaperones Hfq and ProQ. In addition, the few identified cases of trans-encoded sRNA-mediated regulation suggest that in *H. pylori* these mechanisms deviate from those of the model Gram-negative organism *E. coli*.

NikS

NikS/HPnc4160 (previously named IsoB) is a ~130 nt highly conserved sRNA transcribed antisense to the small ORF encoding *aapB*. NikS was identified for the first time as a part of a degenerated type I TA system, as the expression of the predicted *aapB* mRNA on the complementary strand was barely detectable in 26695 and G27 strains (Sharma *et al.,* 2010; Vannini *et al.,*2017).

NikS was found to target genes encoding primary colonization and virulence factors, including the carcinogenic oncoprotein CagA, the vacuolating cytotoxin VacA and a spectrum of outer membrane proteins comprising adhesins. Eisenbart and co-workers demonstrated the translation inhibition following NikS binding to the 5'UTR of *cagA*, *vacA*, *hofC*, HP1286 and *horF* transcripts (Eisenbart *et al.,* 2020). However, another study has demonstrated the interaction of this sRNA with other sequences of *cagA* transcript, a result that underlined differences or unproper characterization of the NikS regulatory mechanism (Kinoshita-Daitoku *et al.,* 2021).

The expression of NikS is under the control of a two layered system. NikS is transcriptionally regulated by the transcriptional regulator NikR, that represses the NikS transcription in response to increasing nickel concentrations (Vannini *et al.,* 2017; Eisenbart *et al.,* 2020). In addition, variations in the length of the T-stretch upstream of the -10 box of the NikS promoter influence the sRNA expression probably by changing the distances of promoter elements and, in turn, RNA polymerase binding efficiency (Kinoshita-Daitoku *et al.,* 2021). In contrast to mouse and gerbil colonization models, in vitro cultures of the *H. pylori* ATCC 43504 strain did not report variations in the T-stretch length over prolonged culture time. The phase variable NikS regulation was proposed to be modulated by stress conditions related to host infection.

RepG

The Regulator of Polymeric G-repeats (RepG/HPnc5490) was found to be one of the most abundant transcripts in the 26695 *H. pylori* strain (Sharma *et al.,* 2010). It is an 87 nt long trans-acting sRNA transcribed in the intergenic region between genes encoding for the essential orphan response regulator HP1043 and the membrane metallophosphoesterase HP1044.

RepG sRNA mediates the post-transcriptional regulation of the bicistronic operon *tlpB-HP0102*, encoding for the chemotaxis receptor TlpB and a glycosyltransferase involved in lipopolysaccharide (LPS) O-chain biosynthesis. This sRNA acts in a non-canonical way by targeting a phase-variable G-stretch in the 5'-UTR of the *tlpB-HP0102* operon. Depending on the length of the G-repeat, RepG can mediate either the translational activation or repression of the *tlpB-HP0102* operon (Pernitzsch *et al.,* 2014). This peculiar characteristic enables a gradual

rather than ON/OFF switch of the expression of these targets, allowing the bacterium to explore different target levels towards the better conditions to evade the host immune response and resist to membrane-targeting antibiotics (Pernitzsch *et al.,* 2021).

CncR1

The *cag*-PAI Non-Coding RNA 1 (CncR1/HPnc2630) is a trans-acting highly conserved (~95%) sRNA encoded in the 5' UTR of *cagP* ORF in the cag pathogenicity island (*cag*-PAI) (Sharma *et al.,* 2010). The expression of CncR1 is under the control of the P_{cagP} promoter and is regulated in a growth-dependent way by the essential orphan response regulator HP1043 (Vannini *et al.,* 2016). Indeed, DNase I footprint assays revealed a protection region from position -19 to -43 from the *cagP* transcriptional start site for HP1043.

The transcriptome analysis of a *cncR1* deletion mutant (Δ*cncR1*) revealed that 71 genes were differentially expressed. Among these, a group of genes involved in the regulation and assembly of the flagellar apparatus (including the flagellar hook length control protein FliK) and whose transcription is governed by the alternative σ^{54} factor RpoN were upregulated. The transcriptome analysis further pointed out the downregulation of mRNA levels of several membrane proteins in the Δ*cncR1* strain, including the adhesion factors SabA and fibronectin/fibrinogen-binding protein HP1392. In accordance, Δ*cncR1* mutant showed a hypermotile phenotype but with reduced capacity to adhere to human gastric adenocarcinoma cells in vitro compared to the wild type.

CncR1 was further demonstrated to establish atypical interactions with the *fliK* transcript in vitro. As revealed from EMSA and RNase T1 footprint experiments, CncR1 binds to several regions along the coding sequence (CDS) of the *fliK* transcript (Vannini *et al.,* 2016).

In conclusion, CncR1 is deeply involved in modulating *H. pylori* virulence through opposite effects on motility and adhesion to host cells.

1.4 Ribonucleases (RNases) mediated post-transcriptional regulation

The control over RNA decay is a strictly regulated process that allows bacterial cells to rapidly react to changing environmental conditions. Endo- and exo-ribonucleases (RNases) are nucleolytic enzymes involved in the degradation and maturation of different RNA species (i.e., mRNAs, tRNAs, rRNAs and ncRNAs) and act as critical factors in post-transcriptional regulation. The RNase enzyme machinery is highly variable in composition and numbers among different bacterial species; orthologous enzymes frequently show different spectra of action depending on factors such as the nature of the bacterium or the redundancy degree of the

genome. For instance, *E. coli* possesses 15 RNases, including the essential RNase E, which is involved in the processing or turnover of all classes of RNAs (i.e., mRNAs, 16S and 5S rRNAs, tmRNAs and tRNAs) (Mackie, 2013). The Gram-positive model *B. subtilis* lacks an RNase E orthologue but retains both the functionally related RNase J1/J2 and RNase Y (considered the functional equivalent of RNase E from *E. coli*) among the 20 different RNases it expresses (Durand and Condon, 2018).

H. pylori is equipped with a constrained RNase apparatus, strikingly similar to that of Gram-positive bacteria. In accordance with the low redundancy degree of its small genome, this bacterium expresses 8 predicted RNases, including RNase J (HP1430), RNase Y (HP0760), RNase R (HP1248), RNase III (HP0662), RNase P (HP1448), PNPase (HP1213), RNase HI (HP0661) and RNase HII (HP1323). The only two RNases essential for the *H. pylori* viability known to date are RNase P (involved in tRNA maturation) and the endo- and 5'-3' exo-ribonuclease RNase J (Redko *et al.,* 2013). The RNase J play a crucial role in *H. pylori* physiology. Indeed, together with the RhpA DEAD-box RNA helicase, the RNase J constitutes the minimal degradosome of *H. pylori*. These two proteins assemble into foci located at the inner cell membrane and are associated with translating ribosomes, thus coupling mRNA translation and degradation (Tejada-Arranz *et al.,* 2020a). The membrane compartmentalisation of RNA degradosomes has been related to the decay rate of different categories of transcripts, including regulatory sRNAs (Moffitt *et al.,* 2016). The depletion of the RNAse J in the *H. pylori* B128 strain led to a 4-fold increase of 55% of the mRNAs and 49% of the asRNAs. Curiously, few sRNAs encoded from intergenic regions were affected, with only 5 sRNAs increased more than 4-fold, and no role in the maturation of other stable ncRNAs (i.e., tRNAs and rRNAs) was observed (Redko *et al.,* 2016). Accordingly, in *H. pylori* a significant role in the maturation of rRNAs has been attributed to RNase III. This double-strand RNase initiates the rRNAs processing by cleaving two stem-loop structures in the 23S-5S rRNA polycistronic precursor and a stem-loop upstream of the mature 5S sequence. In addition, RNase III cleaves the intermolecular complex formed by the leader region of the 23S-5S precursor and its cis-encoded asRNA (Iost *et al.,* 2019).

The mechanisms regarding the degradation, metabolism and maturation of the sRNAs in *H. pylori* remain almost unknown. IGRs-encoded sRNAs frequently require the action of a single-strand endo-RNase to maturate and expose the seed region, increase their stability or even generate two separate sRNA molecules with distinct regulons. Although in other enterobacteria as *Salmonella enterica* or *E. coli*, this task is almost exclusive of RNase E (Fröhlich *et al.,* 2016; Chao *et al.,* 2017), *H. pylori* and all the Campylobacterota are the only proteobacteria that lack an orthologue of such enzyme (Sharma *et al.,* 2010; Laalami *et al.,* 2014). In addition, the other

single-strand specific endo-RNase represented in the *H. pylori* genome is RNase Y, an enzyme shown to be central in the degrading machinery of pathogens such as *B. subtilis* and *Streptococcus pyogenes* (*S. pyogenes*) (Tejada-Arranz *et al.* 2020b).

1.4.1 RNase Y

The main endo-RNases that participate in the initial step of RNA metabolism in Gram-negative and Gram-positive bacteria are RNase E and RNase Y, respectively (Mohanty and Kushner, 2016). An analysis of the phylogenetic distribution of different endo-RNases conducted by the group of Tejada-Arranz showed that less than 1% of the analysed genomes carried both RNase E and RNase Y, while 26%, including *B. subtilis* and *H. pylori*, express both RNase J and RNase Y (Tejada-Arranz *et al.,* 2020). Of interest, RNase Y is more represented in Gram-positive genomes characterised by a low GC content, while RNase E or RNase G are more frequently represented in high GC Gram-positive genomes (Durand *et al.,* 2015).

The structure and the central role of RNase Y have been mainly examined on Gram-positive pathogens such as *B. subtilis*, *S. pyogenes* and *Staphylococcus aureus* (*S. aureus*). *B. subtilis* RNase Y is characterised by the presence of four major domains. The extended N-terminal α-helical region comprises a short transmembrane domain (residues from 5 to 24) and an intrinsically disordered coiled-coil domain (residues from 30 to 192) and is involved not only in the subcellular localisation of the protein, but also in its oligomerisation (Hamouche *et al.,* 2020). In addition, the coiled-coil domain works as a scaffold for the assembly of a functional RNA degradosome complex with the DEAD-box RNA helicase CshA, the RNase J1/J2, the PNPase, the phosphofructokinase PfkA and the enolase proteins (Lehnik-Habrink *et al.,* 2010). The C-terminal region instead shows a globular structure. It harbours a type 1 K-homology domain (KH domain) (residues from 210 to 280), involved in RNA recognition and binding, and a catalytic HD domain (Lehnik-Habrink *et al.,* 2011).

RNase Y has been shown to cleave preferentially 5’ monophosphorylated single stranded RNA (Shahbabian *et al.,* 2009). The analysis of the 5’ end of the processed transcripts generated following RNase Y cleavage further revealed the presence of a G located upstream of the processing site in 58% and 87.4% of target RNAs in *S. aureus* and *S. pyogenes*, respectively (Broglia *et al.,* 2020; Chen *et al.,* 2013). However, this prerequisite was not reported in *B. subtilis*. Indeed, in this bacterium and *S. aureus*, RNase Y seems sensitive to the RNA secondary structure downstream of its cleavage site (Shahbabian *et al.,* 2009; Marincola *et al.,* 2017).

Depending on the bacteria, different roles have been attributed to RNase Y. In *B. subtilis*, RNase Y is the principal responsible for RNA degradation, as its deletion increases the bulk mRNA half-life by more than 2-fold (Durand *et al.*, 2012). In addition, RNase Y is involved in the maturation of different RNA classes, such as riboswitches (Shahbabian *et al.*, 2009), the ribozyme RNase P (Gilet *et al.*, 2015), and polycistronic mRNAs (DeLoughery *et al.*, 2018). Nevertheless, such solid activity was not reported for *S. aureus* and *S. pyogenes*, where only a limited but exclusive number of direct targets has been identified (Khemici *et al.*, 2015; Broglia *et al.*, 2020).

2. Aim

H. pylori is one of the most widespread and successful human pathogens. This bacterium colonizes the human gastro-intestinal tract (i.e., the only known reservoir) of almost half of the world's population and its infections commonly persist throughout life. The capacity of *H. pylori* to adapt to the restricted host-associated environment and to evade the host immune response largely depends on its streamlined and efficient signalling network (Mo *et al.*, 2022). Regardless the constrained number of transcriptional regulators, in the last few years a fundamental role in the control of gene expression has been attributed to post-transcriptional regulatory mechanisms including sRNAs (Sharma *et al.*, 2010). However, among the 8 RNases represented in *H. pylori* genome, a regulator guiding sRNAs metabolism is still not well defined (Redko *et al.*, 2016).

In the presented Ph.D. project, we investigated the physiological role in *H. pylori* G27 strain of the RNase Y enzyme.

To do this, we followed three major research lines. In the first one we provide a comprehensive characterization of the RNase Y activity by analysing its genomic organization and the factors that orchestrate its expression. Then, based on bioinformatic prediction models, we depict the most relevant determinants of RNase Y function, demonstrating a correlation of both structure and domain organization with orthologues represented in Gram-positive bacteria. To unveil the post-transcriptional regulatory effect exerted by the RNase Y, we compared the transcriptome of an RNase Y knock-out mutant to the parental wild type strain by RNA-seq approach.

In the second line of research we characterized the activity of this single strand specific endoribonuclease on *cag*- non-coding RNA 1 (cncR1), a *trans*-acting sRNA involved in the programmed expression of motility and adhesion genes.

Finally, we focused on the characterization of the *in vivo* interactome of CncR1. We set up a preliminary MS2-affinity purification coupled with RNA-sequencing (MAPS) approach and we evaluated the enrichment of specific targets, demonstrating the suitability of the technique in the H. pylori G27 strain.

3. Results

3.1 PART I: Characterization of RNase Y

3.1.1 RNase Y genomic locus

Differently from many other bacterial genomes, *H. pylori* was previously thought to lack an extensive operon organization of its ORFs (Thompson *et al.*, 2003). However, the primary transcriptome analysis of *H. pylori* 26695 strain evidenced a consistent polycistronic organization of the genome, as 87.5% of all *H. pylori* genes were shown to belong to 337 primary operons (Sharma *et al.*, 2010). Among these, the genes encoding for RNase J (HP1430), RNase R (HP1248), RNase P (HP1448), PNPase (HP1213), and RNase HII (HP1323) were confirmed as members of distinct operons, while RNase HI (HP0661) and RNase III (HP0662) forms a unique transcriptional unit. In addition, this analysis identified *rny* gene (HP0760), encoding for RNase Y, and HP0761 as part of a same bicistronic transcriptional unit under the control of the P_{761} promoter.

The genomic organization of HP0761 and *rny* genes in *H. pylori* G27 resembles that observed in 26695 strain, as the two annotated coding sequences (CDSs) show a tandem orientation and an overlap of 101 bp. In addition, the analysis of their genomic loci revealed the presence of two AAGGag-like Shine-Dalgarno sequences (light grey square in Fig 1B) 8 bp and 6 bp upstream HP0761 and *rny* start codons respectively. However, a single transcriptional start site (TSS) upstream HP0761 was identified in (Sharma *et al.*, 2010) and a TATAAT -10 box (dark grey square) identical to the σ^{80} consensus sequence was detected upstream the TSS.

To validate the hypothesis that in G27 strain HP0761 and *rny* are co-transcribed as a bicistronic operon, we set up a semiquantitative PCR (RT-PCR) analysis. A sample of G27 wild type (WT) culture was employed for total RNA extraction followed by cDNA synthesis. Two sets of retrotranscription reactions, i.e., with (RT+) or without (RT-) the reverse transcriptase enzyme, were made to exclude a potential contamination by residual genomic DNA. Employing these templates, two genomic regions were assayed: a first region (A1) encompassing part of HP0761 and *rny* CDSs and their overlapping sequences, and a second region (A2), used as negative control, spanning from HP0761 to HP0762 gene which is under the control of the divergent promoter P_{762}. An amplicon generated on the 16S rRNA transcript was included as positive control of the reaction. In accordance with the transcriptome analysis previously performed in 26695 strain (Sharma *et al.*, 2010), the appearance of a strong signal

corresponding to the A1 amplicon and the absence of the A2 amplicon suggest that HP0761 and *rny* are transcribed as a single transcriptional unit.

The P_{761} promoter was further characterized: a primer extension analysis was performed to validate the TSS upstream the HP0761-*rny* operon and a Sanger sequencing reaction was added to map the TSS. The TSS (bent arrow in Fig. 1D) was mapped 22 bp upstream of the annotated start codon of the HP0761 CDS (black triangle in Fig. 1D), coherently with the *H. pylori* 26695 annotation. An additional prominent fast migrating band (indicated by an asterisk in Fig. 1D) was detected on the autoradiographic film. Although this band could arise from a non-specific hybridization of the primer probe, another speculative but intriguing hypothesis is that it could correspond to a shorter HP0761-*rny* transcript, possibly processed by a single strand specific endoribonuclease (ssRNase) or other RNases.

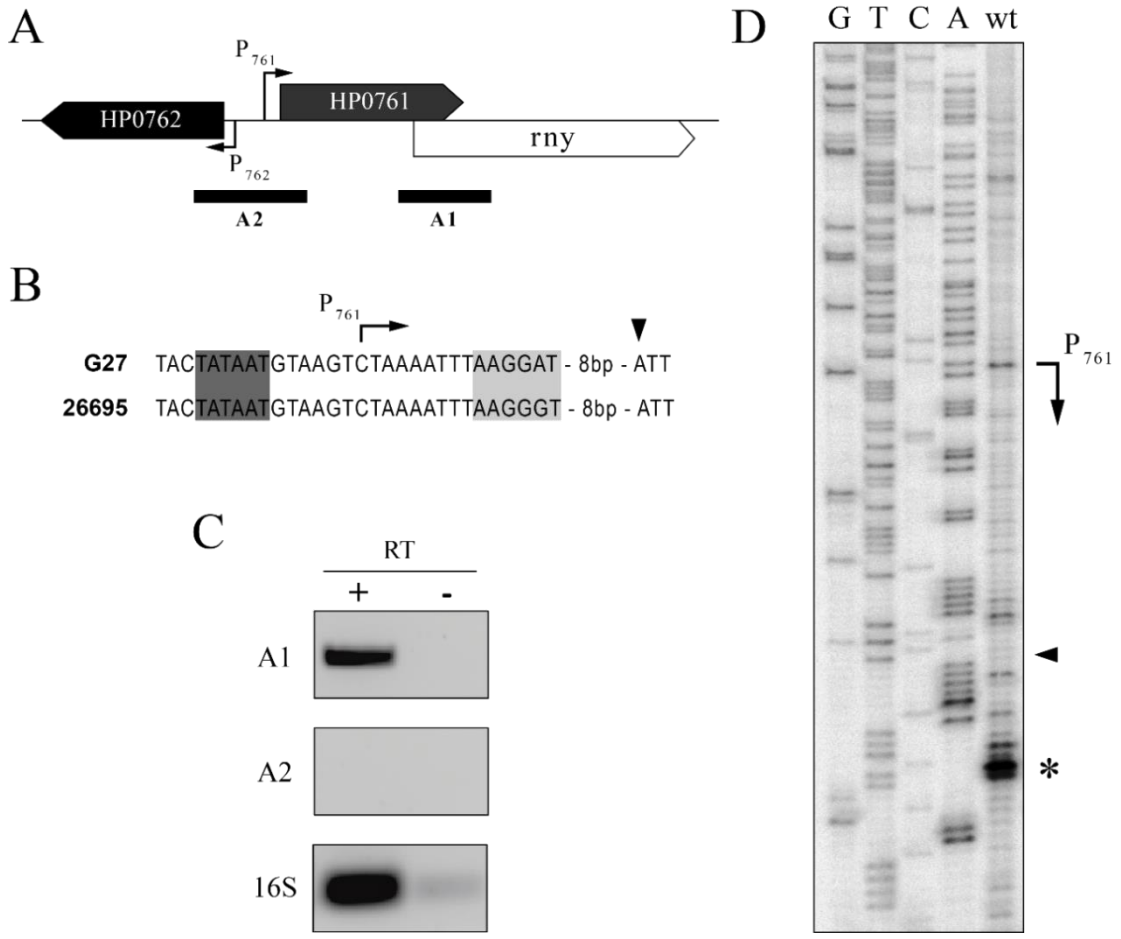

Figure 1: **A**) Genomic organisation of the HP0761-*rny* operon in *H. pylori* G27 strain. Bent arrows indicate the transcription start sites (TSSs). The position of the amplicons of the RT-PCR analysis (panel C) are indicated by black bars. **B**) Nucleotide sequence and relevant features of the P_{761} promoter: -10 region and Shine-Dalgarno sequence are embed in dark grey and light grey boxes, respectively. P_{761} TSS (derived from dRNA-seq analysis [Sharma *et al.*, 2010] and start codon are indicated by a bent arrow and a black triangle respectively. **C**) RT-PCR analysis of transcript at different positions of HP0761 gene: straddling HP0761 and *rny* (A1, generated with oligos 716-F and 717-R) and encompassing HP0761 and the divergently oriented HP0762 (A2, amplified with oligos 717-F and 718-R). A positive control generated on the 16S transcript (amplified with oligos 16S-RTF and 16S-RTR) was included.

D) Primer extension analysis performed on *H. pylori* G27 strain. Primer extension and Sanger sequencing reactions were loaded to map the TSS (bent arrow) of the HP0761-*rny* transcript. Black triangle indicates the annotated HP0761 start codon. An asterisk marks the second major band of the primer extension reaction.

3.1.2 Fur and Fe^{2+} dependent regulation of P_{761}

The inspection of the P_{761} promoter revealed a TCATT-n12-TT sequence spanning from -70 to -51 upstream of the TSS that is similar to the TCATT-n10-TT consensus sequence proposed for *apo*-Fur (Vannini *et al.*, 2022). Fur is a well-known transcriptional regulator (TR) that modulates the expression of the targeted genes in response to iron levels. When iron is scarce, apo-Fur is the predominant form of the TR and it regulates its apo-regulon. The observation of the apo-Fur consensus sequence within P_{761} suggested a possible Fur-dependent transcriptional regulation of the HP0761-*rny* operon in response to iron levels. Since the intracellular levels of the Fur protein increases in the late-exponential phase of growth (Danielli *et al.*, 2006), we harvested bacterial cells grown to an OD_{600} = 1.0-1.1 of the *H. pylori* G27 wild type and Δ*fur* strains, with the latter harbouring a knock-out deletion of *fur* (Delany *et al.*, 2001). Total RNA was extracted and cDNAs were synthesised after the depletion of genomic contaminant DNA. Transcript levels of the *rny* gene were finally assayed by quantitative real time PCR (RT-qPCR).

In the wild type strain, a 2.4 fold increase of the *rny* mRNA levels was detected in samples treated with an iron chelator (20 min, 150 μM 2,2′-Dipyridyl) compared to cells treated with iron (20 min, 1 mM $(NH_4)_2Fe(SO_4)_2$). In contrast, no significant variations in the *rny* transcript levels were observed when the same treatments were performed on the Δ*fur* strain (Fig. 2B). Hence, *rny* mRNA levels were regulated in response to iron levels, and Fur appeared to mediate the Fe^{2+}-dependent regulation, likely binding to the P_{761} promoter.

To validate the interaction of Fur with the P_{761} promoter predicted by the presence of the consensus sequence and to map the DNA region bound by Fur, we set up DNase I footprinting assays. Increasing amounts of the recombinant Fur protein were incubated with a DNA probe corresponding to the P_{761} promoter in Fe^{2+}-depleted (*apo*-Fur) and Fe^{2+}-repleted (*holo*-Fur) conditions, then we proceed with the digestion with DNaseI. As reported in Fig. 2A, *apo*-Fur showed two regions protected by nuclease digestion on the P_{761} probe, spanning from position -71 to -60 and from -55 to -40 with respect to the TSS and overlapping with the *apo*-Fur consensus sequence. Interestingly, the DNA regions protected by *apo*-Fur appeared at the lowest concentration tested of the protein (8.3 nM of *apo*-Fur), indicating a high affinity of apo-Fur for the P_{761} promoter. In contrast, the DNaseI footprinting assay of Fur on the P_{761} probe performed in presence of iron (*holo*-Fur) revealed a single region of protection from position -

71 to -60 with respect to the TSS. Although the *holo*-Fur region of protection corresponded to one of the two regions protected by *apo*-Fur, *holo*-Fur showed lower affinity to the probe than *apo*-Fur, as the protection was detectable only at the highest (224 nM) concentration tested. Both experiments revealed the presence of a DNase I-hypersensitive site (indicated by a triangle, Fig. 2A).

The high-affinity binding sites of *apo*-Fur on the P_{761} promoter are in positions that are compatible with a positive effect exerted by Fur on the transcription of the HP0761-*rny* operon, oppositely to the classical apo-Fur repression in which the Fur binding sites invariantly overlap the core promoter of the targeted genes. These results are consistent with those obtained with the RT-qPCR analysis and support the hypothesis of an *apo*-Fur mediated induction of the P_{761} promoter in response to low iron levels.

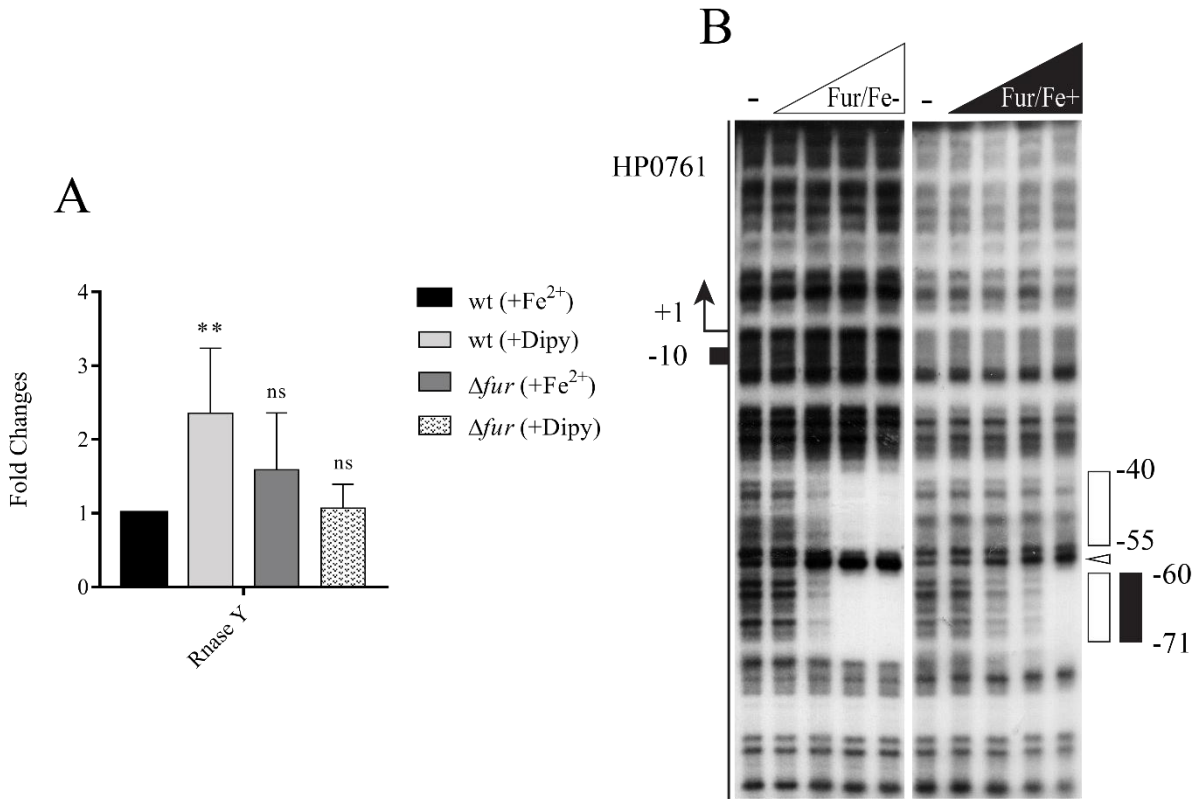

Figure 2: **A**) DNase I footprinting assay. A probe generated on the P_{761} promoter, radiolabeled on the non coding strand, was incubated with increasing concentrations (0, 8.3, 25, 75 and 224 nM) of purified Fur protein in Fe^{2+}-depleted (left) or Fe^{2+}-repleted (right) conditions. On the right, the white and black boxes indicate the DNA regions of P_{716} protected by apo- and holo-Fur by DNaseI digestion, while the white triangle indicates a DNase I hypersensitive site. **B**) Quantitative PCR (RT-qPCR) analyses of transcript levels at the *rny* gene. Oligonucleotides specific for 16S (16S-RTF/16S-RTR) and *rny* (RNaseY-RTF/RNaseY-RTR) were used. Ct values were normalized on the 16S internal control and gene expression is reported as n-fold variation with respect to the wild type ($+Fe^{2+}$) strain. Mean values from at least 3 biological replicates are reported with vertical bars indicating standard deviation. The statistical significance (asterisks) was calculated with One-way ANOVA test as: ns = not significative * = p-value < 0.05; ** = p-value < 0.01; *** = p-value < 0.001; **** = p-value < 0.0001.

3.1.3 Prediction of RNase Y functional domains

The extensive analysis performed by Tejada-Arranz and co-workers on bacterial degradosomes revealed that 26% of the 1535 bacterial genomes analysed (including *Bacillus subtilis* and *H. pylori*) lack an RNase E ortholog but encode for both RNase Y and RNase J (Tejada-Arranza *et al.,* 2019). In the Gram-positive *B. subtilis* the essential RNase Y was shown to be fundamental in the mRNA catabolic processes.

As a first step in the characterisation of the RNase Y enzyme in *H. pylori* G27, we used InterPro, DeepTMHMM and Phobius tools to carry out an *in silico* prediction of the functional domains. The structural analysis of the 529 amino acids of the RNase Y sequence revealed the presence of an N-terminal transmembrane domain (residues 5 to 26), a central KH (residues 225 to 297), and HD (residues 342 to 415) domains. The importance of the transmembrane domain, which is predicted to cross the bacterial membrane with a single α-helical motif, is further supported by the membrane localisation of the RNase Y orthologues in other bacteria, such as *B. subtilis* (Hamouche *et al.,* 2020). The KH domain is a single-stranded, sequence-specific RNA binding domain characterised by a minimal β-α-α-β core structure. The ability to bind the nucleic acid backbone lies in a conserved G-x-x-G motif (identified in the residues 233-236, Fig. 3C) that links the two α helices of the minimal core (Nicastro *et al.,* 2015). The HD domain instead was predicted to be the catalytical domain. Considering the high conservation degree in the *Helicobacter* genus, we identified the His-Asp couplet in position 374-375 as the Zn^{2+} and Mg^{2+} metal-chelating residues that could coordinate the RNase Y phosphohydrolytic activity (Aravind *et al.,* 1998).

The analysis performed with Marcoil bioinformatic tool additionally predicted the presence of a coiled-coil domain from residues 73 to 140 with high (>80%) probability (Fig. 3B). In particular, the hydrophobic residues V104, L111, L118, L125 and F132 are aligned on the same side of the α-helix and have the potential to form a leucine zipper motif which could promote the dimerization of the protein. Consistently, the mutual interaction of the positively and negatively charged residues placed on the lateral side of the α-helix can further stabilize the leucine zipper. The same analysis performed with Parcoiled2 confirmed the previous prediction, as a coiled coil domain is predicted with high (>90%) probability for the α-helix portion which includes residues 106 to 140.

H. pylori RNase Y has only a 38.8% of aminoacidic sequence conservation with its orthologue in *B. subtilis*. In both bacteria the RNase Y functional domains have a similar organization, with an N-terminal transmembrane helix followed, in order, by a short coiled-coil domain, a KH ssRNA binding domain, a catalytical HD motif and a C-terminal domain with unpredicted function. This observation suggests a correlation among their role in the cell.

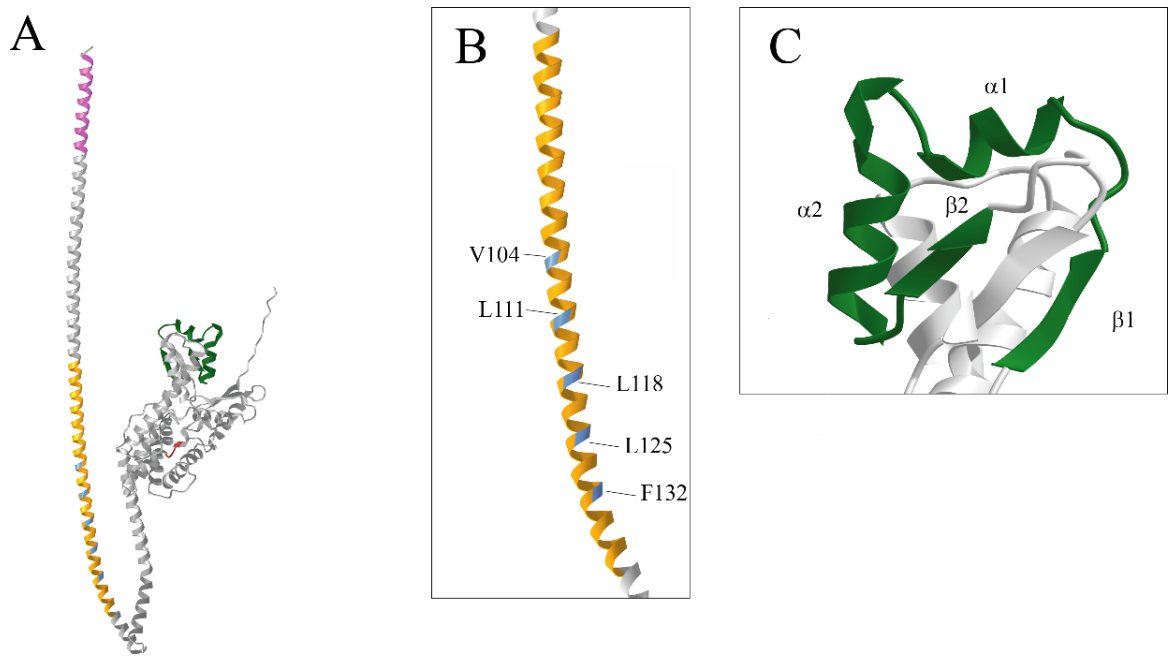

Figure 3: **A**) *H. pylori* RNaseY structure predicted with the AlphaFold computer program(Jumper *et al.*, 2021; Varadi *et al.*, 2022). Predicted functional domains are evidenced in different colours: transmembrane α-helix (pink), coiled coil (orange), KH-type I (green) and HD motif (red). **B**) Inset on the coiled coil structural domain. The V104, L111, L118, L125 and F132 residues, which constitute the leucine zipper motif, are highlighted in light blue. **C**) β-α-α-β core structure of the KH-type I (ssRNA-binding) domain.

3.1.4 Characterization of RNase Y predicted catalytic HD domain

To investigate the role exerted by RNase Y in *H. pylori* physiology, we generated a *rny* knock-out mutant. To this purpose, *H. pylori* G27 was transformed with the PCR product *rny*-UP::KmR::*rny*-DOWN, in which most of the *rny* CDS was replaced with the kanamycin resistance gene, leaving the upstream HP0761 gene intact (Fig. 4A). The correct insertion of the KmR gene in the resulting Hp G27 Δ*rny* mutant was confirmed by PCR. To further determine the importance of the His-Asp residues of the predicted catalytic domain, Δ*rny*::*rny* (ectopically expressing the wild type *rny* sequence) and Δ*rny*::rny_{H374A} (carrying an H374A point mutation in the ectopic *rny* sequence) complemented strains were generated from the *rny*-null background. In both mutants, the region encompassing the HP0761-*rny* operon under the control of the native P_{761} promoter was cloned in the *vacA* locus as reported in Fig. 4A. Moreover, to avoid the presence of two functional genomic copies of the HP0761 gene, its ectopic copy in the complemented sequence carried an in-frame deletion.

Then, we assayed the *rny* expression levels in all the generated mutants by performing RT-qPCR on RNAs extracted from mid-exponentially growing liquid cultures. As shown in Figure 4, the Δ*rny* knock-out mutant showed a complete loss of *rny* expression, while the

complemented Δ*rny*::*rny* strain exhibited *rny* levels similar to wild type strain, suggesting that the insertion of the *rny* sequence in the *vacA* locus fully restored the expression of *rny*. Moreover, the partial deletion of the upstream-transcribed HP0761 sequence did not compromise the *rny* expression in the complemented mutant. Interestingly, when the bacterium expresses a RNase Y enzyme mutated in its predicted catalytic site, the *rny* transcript strongly accumulates (up to 7-fold) compared to the wild type(Fig. 4B, hatched column).

Then, to assess the effects exerted by the different *rny* mutants on the bacterial fitness, we determined their growth rate during the exponential phase of growth by measuring optical density at 600 nm (OD_{600}). The generation time of each strain was calculated by the following formula:

$$\text{generation time} = \frac{\text{Duration} \cdot \ln_2}{\ln(\frac{OD_f}{OD_i})}$$

The Δ*rny* strain showed an impaired growth compared to the WT, as the generation time increased by ~30% from 2.75 ± 0.15 h (wt) to 3.57 ± 0.41 h (Δ*rny*), suggesting that the absence of RNase Y has a moderate impact on *H. pylori* fitness and physiology (Fig. 4C, left panel). Although the rate of growth of Δ*rny*::*rny* complemented strain resembled that of the wild type (2.73 ± 0.03 h), the expression of the RNase Y carrying the H374A mutation (Δ*rny*::*rny*^{H374A}) reduced the growth rate (3.39 ± 0.12 h), seemingly having a fitness cost similar to that observed for the Δ*rny* strain (Fig. 4C, right panel).

Taken together, these results suggest that the His residue in position 374 could be fundamental for the RNase Y activity and that its mutation likely lead to an inactive phenotype of the protein. The hampered phosphohydrolitic activity of *rny* due to the H374A mutation is also sustained by the increase of the *rny* transcript in the Δ*rny*::*rny*^{H374A} strain. Indeed, negative autoregulation of RNases on their own transcripts is a typical and widespread posttranscriptional control mechanism observed in different bacteria (Jain and Belasco, 1995; Matsunaga *et al.*, 1997; Schuck *et al.*, 2009; Lim *et al.*, 2015), and the accumulation of the transcript likely indicate the loss of autoregulation due to the production of a non-functional protein.

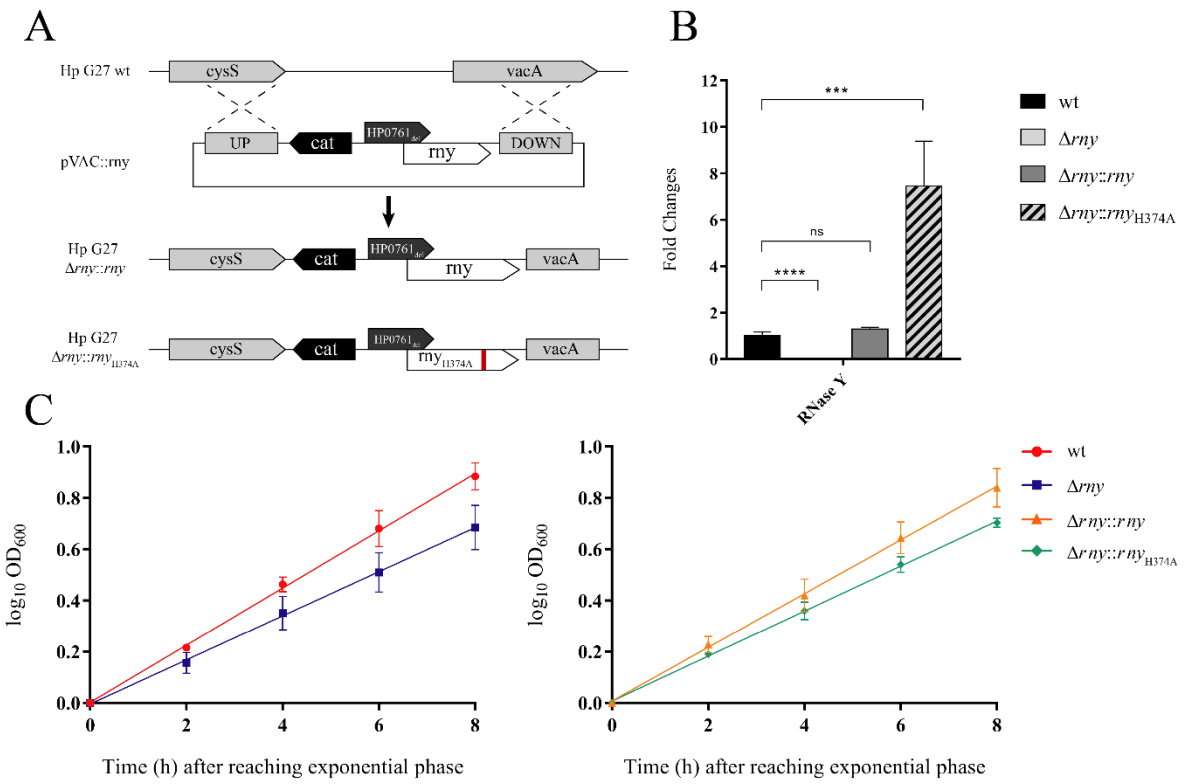

Figure 4: **A**) Schematic representation of the procedure employed to obtain the Δ*rny*::*rny* and Δ*rny*::*rny* ^{H374A} complemented strains. The pVAC::CAT-*rny* vector carrying the 539 bp "UP" region of homology with the *cysS* (HP0886), the 745 bp "DOWN" region of homology with the sequence of *vacA* (HP0887), the *cat* cassette and a 2085 bp fragment encompassing P_{761} promoter, HP0761 carrying an in-frame deletion and wild type or H374A mutated *rny* gene, was used to transform the G27 Δ*rny* strain. The red bar in the G27 Δ*rny*::*rny* ^{H374A} map represent the H374A mutation. **B**) RT-qPCR analysis of *rny* transcript levels. Ct values were normalized on the 16S internal control and gene expression is reported as n-fold variation with respect to the wild type strain. Mean values from at least 3 biological replicates are reported with standard deviation error vertical bars. The statistical significance (asterisks) was calculated with One-way ANOVA test. **C**) Fitness assessment of different mutants and wild type strain by measurements of optical density at 600 nm (OD_{600}) during exponential growth phase. $Log_{10}(OD_{600})$ is plotted against the time after reaching the exponential phase and linear regression was calculated. The graphs report the results of at least three different independent experiments. Mean values from three biological replicates are reported, ± standard deviation; statistical significance was calculated by One-way ANOVA test and expressed as ns = not significative * = p-value < 0.05; ** = p-value < 0.01; *** = p-value < 0.001 ; **** = p-value < 0.0001.

3.1.5 Characterization of RNase Y transmembrane domain

Membrane localisation of the degradosomal apparatus reflects the compartmentalisation of RNA catabolic process, allowing a posttranscriptional regulation of a specific subcategory of genes (Tejada-Arranz *et al.*, 2020).

Since a transmembrane domain was predicted at the amino acid (aa) 5 to 26 of the RNase Y sequence in *H. pylori* (Fig. 3A), we wanted to verify the RNase Y subcellular localisation using a cellular fractionation protocol. This method allowed the separation of the cytoplasmic soluble (Cs), inner membrane (IM), and outer membrane (OM) fractions from a total extract (TE) of lysed bacterial cells by multiple ultracentrifugation steps with increasing concentrations (0, 0.1

and 1%) of the surfactant N-lauroylsarcosine. The proper separation of the cellular fractions was validated by western blots analysis, detecting the HP1043 and BabA proteins that localize in the cytoplasmic soluble and outer membrane fractions, respectively.

Starting from an RNase Y knock-out background (Δ*rny*), we designed a complemented mutant expressing a full-length RNase Y fused at the C-terminal with a FLAG-tag epitope (Δ*rny*::*rny*-FLAG). Western blot analysis performed using a specific α-FLAG antibody showed that most of the RNase Y protein is membrane bound but, surprisingly, is localised on the outer membrane, whereas it was barely detectable in the inner membrane fraction (Fig. 5, bottom left panel). No protein was detected in the cytoplasmic soluble fraction. To further assess the functional properties of the N-terminal transmembrane domain of RNase Y, we expressed a FLAG-tagged RNase Y protein deleted for the transmembrane region (aa 1-26) (Δ*rny*::*rny*ΔTM-FLAG). Unfortunately, the Western blot analysis did not reveal the presence of the truncated RNase Y protein in the total extract, nor in any of the fractions, suggesting that protein truncation may lead to an incorrect folding of the protein followed by degradation phenomena (Fig. 5, bottom right panel).

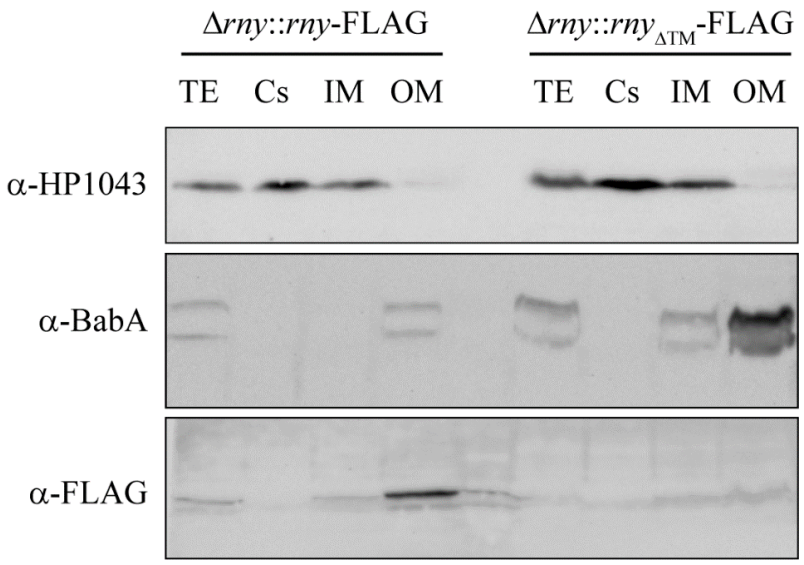

Figure 5: Western blot analysis of the 4 cellular fractions obtained from Δ*rny*::*rny*-FLAG and Δ*rny*::*rny*ΔTM-FLAG mutants. Cellular fractions of *H. pylori* G27 were separated by differential solubilization and ultracentrifugation; in all samples was employed the same amount of proteins (quantification by Bradford). TE, total extract fraction; Cs, cytosolic soluble fraction; IM, inner membrane fraction; OM, outer membrane fraction. Blots were incubated with α-HP1043, α-BabA and α-FLAG antibodies, followed by an incubation with the secondary antibody and ECL development.

3.1.6 Transcriptome analysis of Hp G27 Δ*rny*

To examine the contribution of the RNase Y in the post-transcriptional degradation processes of different RNA classes, we performed a strand-specific transcriptome analysis of *H. pylori* G27 wild type and Δ*rny* strains. Both strains were grown in the same conditions at 37°C until mid-exponential phase (OD_{600} = 0.6) and the results are representative of three independent experiments. *H. pylori* G27 RefSeq annotation (GCF_000021165.1) in the version released on September 2022 was used as the reference for gene annotation to which we manually added validated ncRNAs (i.e., Anti_HsrA, Cncr1, IsoB, Nrr1, Nrr2, sRNAs) (Pelliciari *et al.*, 2017; Vannini *et al.*, 2017).

The analysis showed a total of 68 significantly deregulated genes ($log_2FC > |1|$, *adj p* < 0.01) in the Δ*rny* strain compared to the wild type, with 26 genes down-regulated (including *rny* gene) and 42 genes up-regulated (Fig. 6). According to their cellular function, the *rny*-regulated genes were grouped into distinct functional categories. Among the upregulated genes in the Δ*rny* strain, a cluster of 8 genes, including the chaperonin-encoding *groEL*, strongly contributed to "Post-translational modification, protein turnover, chaperones" category functional enrichment (adj p = 0.002). However, no other functional category was found enriched, nor in the up- neither in the down-regulated genes. This result could be due to both the narrow spectrum of *rny*-dependent genes and the failure to assign 34 of the 68 deregulated genes to any of the functional categories. Despite this, the expression of several representative of Hop/Hor family, including the outer membrane proteins *hopA*, *horL*, the adhesisns *alpA*, *alpB* (log_2FC = 0.97), *hopQ* and the major virulence factor *sabA* adhesin, resulted significantly increased in the Δ*rny* strain. In addition, at least other 4 genes coding for components of major virulence factors were up-regulated upon RNase Y depletion. Among these, the genes encoding the flagellar hook-length control protein (*fliK*), the minor flagellin subunit (*flaB*), the flagellar hook protein (*flgE*) and the urease subunit β (*ureB*) showed 3.6-, 2.2-, 2.1- and 2- fold increase of their mRNA levels.

The transcriptome analysis further revealed that compared to the wild type the expression of ncRNAs overall was not affected in the Δ*rny* strain. Noteworthy, the expression levels of only the CncR1 sRNA were significantly increased in the Δ*rny* strain. The up-regulation of CncR1 is in contrast with the observed increased levels of *fliK*, *flaB* and *flgE*, as the sRNA was demonstrated to oppositely regulate the expression of structural and regulatory flagellar proteins (Vannini *et al.*, 2016).

Overall, this analysis highlights that the RNase Y could be involved in the post-transcriptional control of several *H. pylori* virulence factors involved in the gastric environment adaptation and host-pathogen interaction.

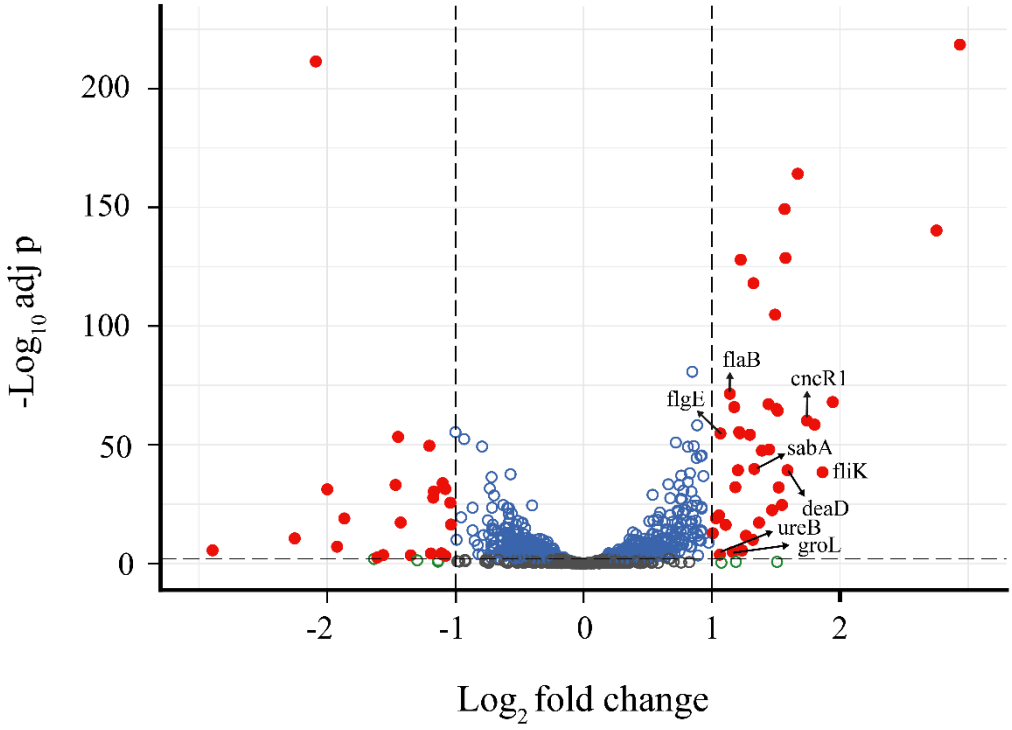

Figure 6: Volcano plot of RNA-seq analysis results. Each point corresponds to the difference in gene expression (Log_2FC; X axis) between Δ*rny* and wild type strains (X axis) plotted against its statistical significance ($-Log_{10}$ adj p; Y axis). Differentially expressed genes (DEGs) are represented with red filled circles when $log_2FC > |1|$, *adj p* < 0.01; empty gray circles correspond to non-differentially expressed genes; empty blue or green circles correspond to genes which $log_2FC > |1|$ or *adj p* < 0.01, respectively. Black dashed lines indicate $log_2FC < 1$, $log_2FC > 1$ and *adj p* < 0.01 threshold values.

3.1.7 RNase Y-mediated regulation of sRNAs

To investigate the possible role exerted by RNase Y in the metabolism of sRNAs, we determined the expression of *cncR1*, *repG* and *nikS* transcripts (3 well known sRNAs of *H. pylori*) in the Δ*rny* mutant strain with respect to the wild type strain. To confirm the specificity of the RNase Y-driven regulation, the same analysis was carried out also in Δ*rny*::*rny* and Δ*rny*::*rny*^{H374A} complemented strains.

Results shown in Figure 7A reveal a significant 6.3-fold increase in the transcript levels of *cncR1* in the Δ*rny* strain (light grey bars) compared to the wild type strain (black bars). The complementation of the knock-out mutant with the wild type *rny* gene locus restored the *cncR1* expression to levels similar to those observed in the wild type (dark grey bars), strengthening the hypothesis of the complementation of the Δ*rny* strain. Interestingly, the Δ*rny*::*rny*^{H374A} strain, expressing a mutated RNase Y protein, showed an up-regulation of *cncR1* transcript similar to that observed in the knock-out. This result further sustains the hypothesis that the *rny*

H374A mutant is non-functional and that His residue in the HD catalytic domain is likely fundamental for the phosphohydrolitic activity of the protein. However, such a regulatory pattern was not detected for *repG* or *nikS*, which showed invariant levels among wild type, knock-out, complemented, and H374A complemented strains.

To understand the effects of CncR1 de-regulation on its regulated targets, we determined the expression levels of CncR1's most well-characterized targets in Δ*rny*, Δ*rny*::*rny* and Δ*rny*::*rny*^{H374A} mutant strains with respect to the wild type. Since it has been shown that CncR1 is involved in controlling flagellar assembly and cell motility (Vannini *et al.*, 2016), our analysis was focused on *fliK* (HP0906), *flaB* (HP0115), *flgE* (HP0870) and *flgB* (HP1559). All selected genes are under the control of the σ^{54} alternative sigma factor and encode for structural (FlaB, FlgE and FlgB) or regulatory (FliK) flagellar proteins.

RT-qPCR analysis revealed significantly increased levels of two of the selected genes, showing 3.3- and 1.6- fold change increases in the Δ*rny* strain compared to the wild type for *fliK* and *flaB* respectively (Fig. 7B). These variations were abolished in the complemented strain, but reappeared with the H374A complemented mutant (Δ*rny*::*rny*^{H374A}).

Curiously, previous analyses reported that CncR1 negatively regulates *fliK, flaB, flgE, flgB* and the other genes within their operons, hence the increases of their transcript levels observed in the RNase Y deficient and inactive strains resembled those observed in the Δ*cncR1* strain. These transcriptional data are in agreement with the wild type vs Δ*rny* results from RNA-seq analysis.

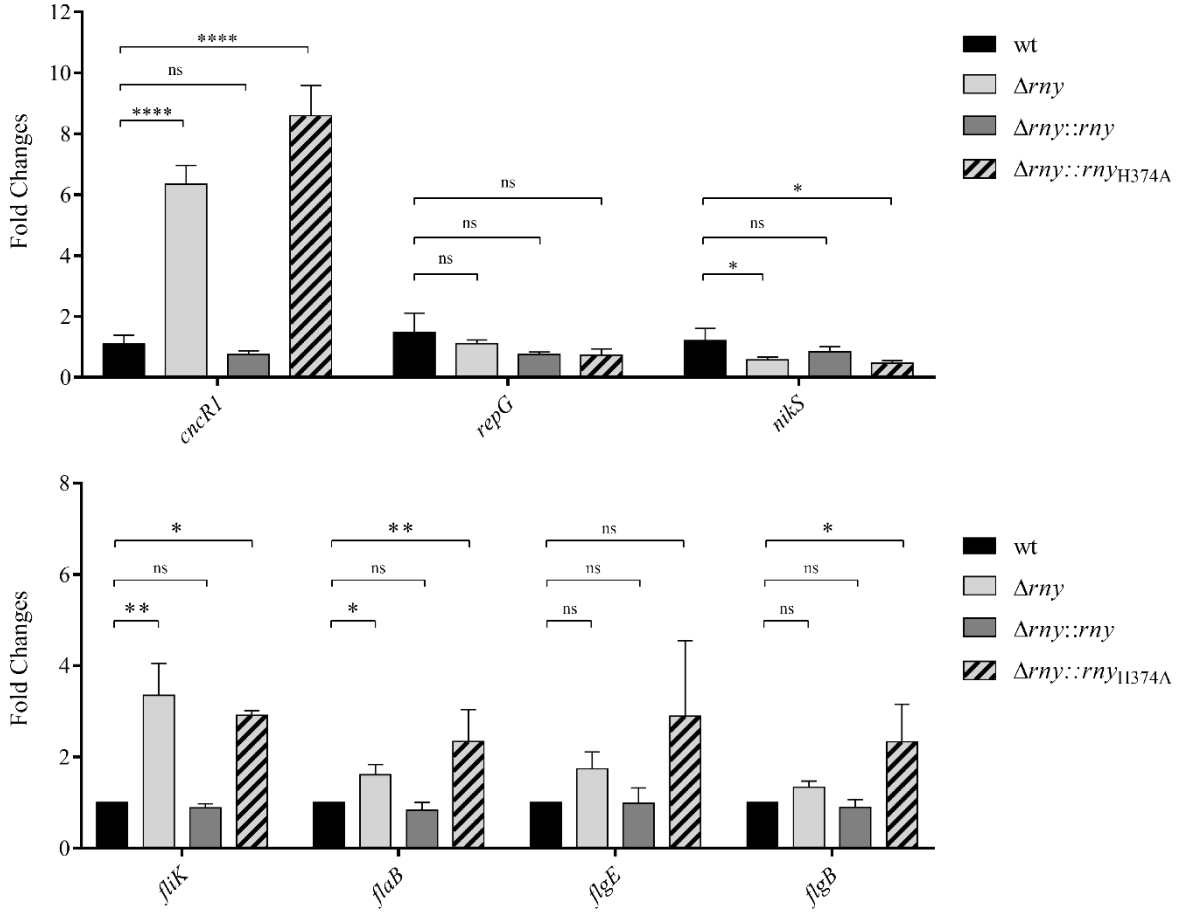

Figure 7: Transcript levels of *cncR1*, *repG* and *nikS*, (panel A) and *fliK flaB*, *flgE*, and *flgB* (panel B) determined by RT-qPCR in *Δrny* (light grey bars), *Δrny::rny* (dark grey bars) and *Δrny::rny*$_{H374A}$ (striped grey bars) mutant strains compared to wild type (black bars) strain. Oligonucleotides pairs 536-RTF/536-RTR (CncR1), RepG-RTF/RepG-RTR (RepG), NikS-RTF/NikS-RTR (NikS), Flik5-RTF/Flik5-RTR (FliK), 115-RTF/115-RTR (FlaB), 870-RTF/870-RTR (FlgE) and 1559-RTF/1559-RTR (FlgB) were used. Ct values were normalized on the 16S internal control and gene expression is reported as n-fold variation to the wild type strain. Mean values from three biological replicates are reported, ± standard deviation; statistical significance was calculated by One-way ANOVA test and expressed as: ns = not significative * = p-value < 0.05; ** = p-value < 0.01; *** = p-value < 0.001 ; **** = p-value < 0.0001.

3.1.8 RNase Y is involved in CncR1 processing

Post-transcriptional regulation mediated by non-coding RNAs (ncRNAs) is emerging to have a fundamental role in the modulation of gene expression in *H. pylori* (Tejada-Arranz *et al.*, 2021), especially considering the small number of transcriptional regulators (only 14) represented in the genome of this bacterium (De La Cruz *et al.*, 2017; Vannini *et al.*, 2022). In this context, the RNases-mediated cleavage of ncRNAs may be crucial for the proper maturation and functioning of these regulators, and examples of the involvement of RNases for the processing, maturation, and activity of different sRNA molecules has been reported (Quendera *et al.*, 2020).

Starting from these observations, we investigated the possible involvement of RNase Y on CncR1 maturation and processing by performing Northern blot experiments on RNA samples extracted from *H. pylori* G27 wild type, Δ*rny*, Δ*rny*::*rny* and Δ*rny*::*rny*^{H374A} strains in the exponential phase of growth (OD_{600} = 0.6-0.7) (Fig. 8). The oligonucleotide 536pe17 (probe 1 in Fig. 8C), mapping at the 5' region of *cncR1*, revealed the presence of the primary *cncR1* transcript (213 nt) in all 4 strains, but an additional transcript with higher molecular weight (>300 nt) specifically accumulates in the Δ*rny* and Δ*rny*::*rny*^{H374A} strains, that correspond to the bacterial strains with a non-functional *rny* gene (Fig. 8B). The same analysis carried out with a probe (probe 2 in Fig. 8A) mapping downstream the terminator confirmed that this band corresponded to a longer RNA transcript. This probe allowed the detection of this transcript in all 4 strains employed for the analysis and it was quantified as 4.1- and 3.6-fold more abundant in Δ*rny* and Δ*rny*::*rny*^{H374A} mutants, compared to the wild type (Fig. 8C).

To get insights into the nature of the CncR1 longer transcript, we looked for alternative TSS that might function in the Δ*rny* and Δ*rny*::*rny*^{H374A} strains compared to wild type and Δ*rny*::*rny* complemented strains. The primer extension assay carried out with probe 1 on the RNAs employed for Northern blot analysis revealed that the *cncR1* TSS is not altered in an RNase Y-deficient background (Fig. 8D). The 5'-end of the *rny* transcript in the three mutant strains was identical to that mapped in the wild type strain, and no additional bands corresponding to alternative TSSs were detected (data not shown). These results indicated that the longer *cncr1* isoform is likely due to differences in the 3'-end of the transcript.

According to the results, we performed a bioinformatic prediction of the secondary structure of the RNA region downstream of the *cncR1* known terminator with RNAfold. The analysis revealed the presence of a stable RNA stem-loop structure (-40.16 KJ/mol) (Fig. 8B) encompassing the positions 300 to 321 from the *cncR1* TSS, i.e. terminating at the 3'-end of the longer *cncR1* isoform. As a typical Rho-independent terminator of transcription is formed by a stem-loop followed by a T-rich sequence, we analysed the 20 nt downstream of the predicted stem-loop structure, but we were unable to detect any T stretch. Nevertheless, the Rho-independent termination in *H. pylori* seems to adopt less stringent criteria compared to the canonical rules designed on the archetype *E. coli* (Castillo *et al.,* 2008). Interestingly, the predicted alternative *cncR1* terminator maps within the *cagP* CDS and no bands corresponding to a full length *cagP* transcript were revealed in the Northern blot analysis. This observation is consistent with previous studies that proposed the loss of expression of a full length CagP ORF (~600 nt) in *H. pylori* G27 (Vannini *et al.,* 2016).

Thus, the *cncR1* longer isoform (from here on cncR1-L) likely corresponds to the transcript arising from the invariant *cagP* TSS and terminating ~321 nt downstream the TSS by the

terminator located at this position. Hence, we hypothesized that a functional RNase Y may process *cncR1*-L isoform to nearly undetectable levels, thus leading *cncR1* shorter isoform (*cncR1*-S) to be the primary product generated from the P_{cagP} promoter.

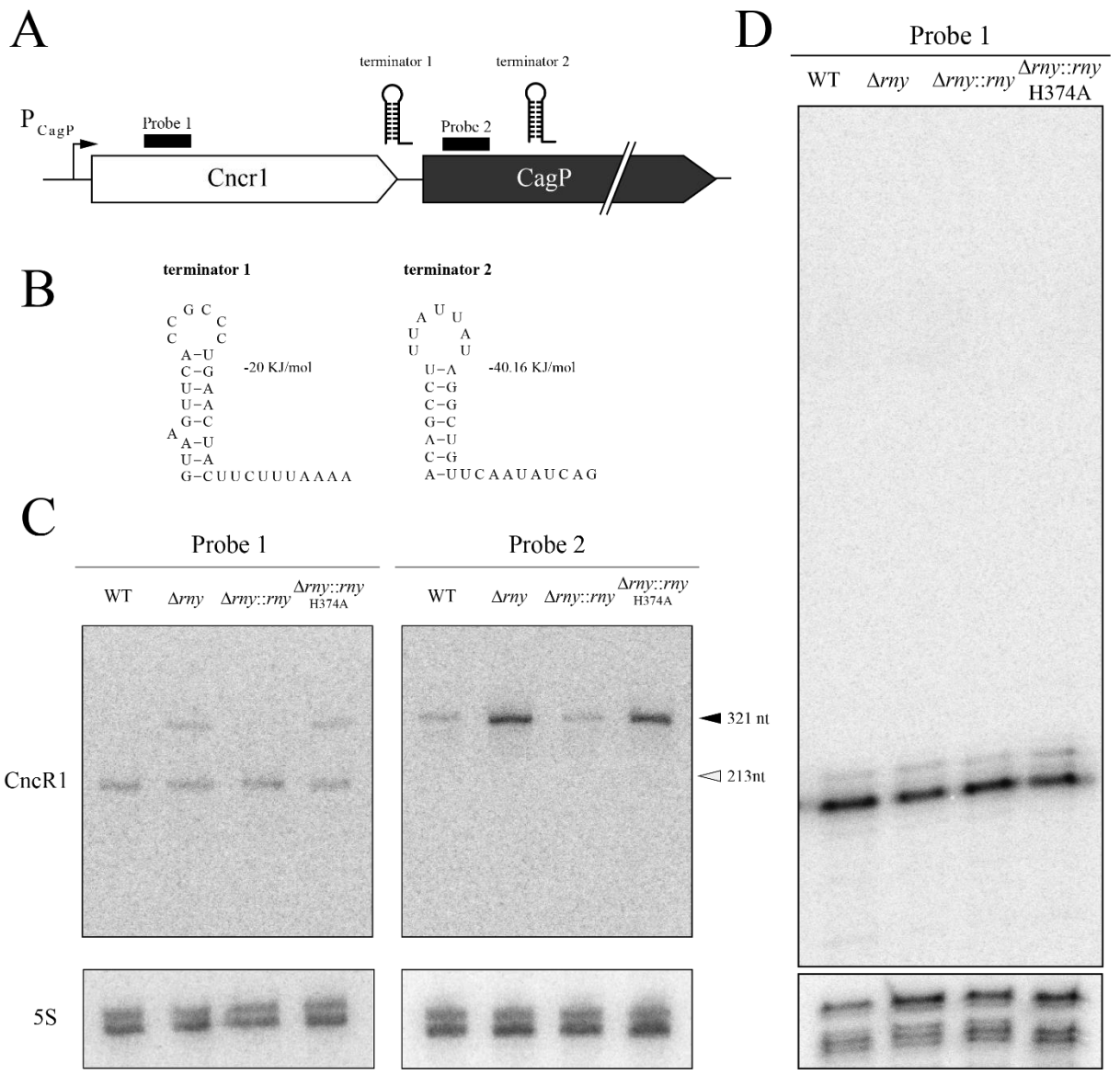

Figure 8: **A**) Schematic representation of CncR1 gene locus in *H. pyori* G27 wild type strain with the primary *cncR1* terminator (terminator 1) and the alternative predicted one (terminator 2). Probes used in Northern blot and primer extensions analyses are represented as black boxes. **B**) Bioinformatic prediction performed of the terminator 1 and terminator 2 secondary structures by RNA-fold. **C**) Northern blot analyses of *cncR1* transcript in G27 wild type, Δ*rny*, Δ*rny*::*rny* and Δ*rny*::rny_{H374A} strains. 536pe17 (Probe 1) and 536pe20 (Probe 2) were employed for the analysis, mapping in the 5'-region of CncR1 transcript and after the terminator 1, respectively. Probe 5S-F annealing to the 5S gene was included as a loading control. White triangle and black triangle indicate *cncR1*-S (213 nt) and *cncR1*-L (>300 nt) transcripts respectively. **D**) Primer extension analyses performed on 20 µg of total RNA extracted from G27 wild type, Δ*rny*, Δ*rny*::*rny* and Δ*rny*::rny_{H374A} strains. 536pe17 oligonucleotide (Probe 1) was used for the reverse transcription reaction. Parallel reactions performed with 5S-F oligonucleotide were used as loading controls.

3.1.9 RNase Y influences the stability of CncR1-L

To establish the impact of RNase Y activity on the maturation of *cncR1* transcript, we determined the stability of both *cncR1*-S and *cncR1*-L isoforms in the wild type and Δ*rny* strains. To inhibit the RNA polymerase activity and, consequently, to block the synthesis of novel transcripts, rifampicin was added to liquid-growing bacteria that reached the mid-logarithmic phase of growth (OD_{600} = 0.6-0.7). Bacterial samples were harvested before (T0) and 2, 5, 10, 15 and 30 minutes after the rifampicin treatment. Northern blot was then performed with the 536pe17 oligonucleotide on the RNA extracted from samples. The stability of the *cncR1-L* isoform (~320 nt), which was barely detectable at T0 in the wild type, was greatly increased in the Δ*rny* strain (Fig. 9, white triangle). This result suggests that in wild type conditions, *cncR1*-L could be rapidly degraded one or more endo- or exo-ribonuclease, including RNase Y. On the contrary, the absence of the RNase Y did not seem to affect *cncR1*-S (black triangle), which appeared slightly more stable in the wild type, thus indicating that *cncR1*-S decay involves an RNase Y-independent pathway maintained in the Δ*rny* strain. Of note, both *cncR1*-S and *cncR1*-L isoforms have shown a comparable degradation rate in the Δ*rny* strain, denoting a possible common mechanism of decay.

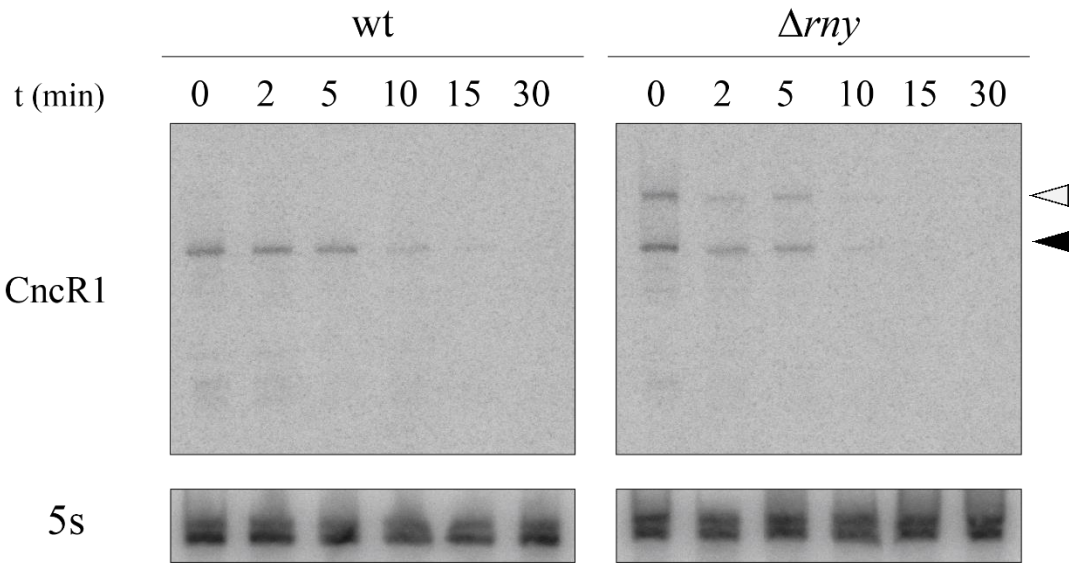

Figure 9: Kinetic analysis of *cncR1*-S and *cncR1*-L stability wild type and Δ*rny* strains. Northern blots were performed with radiolabelled 536pe17 probe on total RNA extracted from G27 wild type and Δ*rny* bacterial cultures untreated (T0) or treated for 2, 5, 10, 15 and 30 minutes with rifampicin. *cncR1*-S (black triangle) and *cncR1*-L (white triangle) correspond to the products with a lower and higher molecular weight, respectively.

3.2 PART II: Preliminary approach to characterize CncR1 interactome

3.2.1 SPECIFIC INTRODUCTION

Non-coding RNAs (ncRNAs) exert a post-transcriptional control on their respective regulatory circuits to influence bacterial physiology and virulence. In the genetic context of *H. pylori*, characterized by a peculiar low number of transcriptional regulators, the *in vivo* determination of trans-encoded targets of the sRNAs is crucial to assess the relevance of this class on ncRNAs as post-transcriptional regulators of gene expression.

Several high-throughput sequencing methods have been designed to unveil comprehensive sRNA – target RNA interaction maps *in vivo*. Many of these techniques take advantage of an RNA-binding protein (RBP), as the widely spread RNA chaperone Hfq or the global small ncRNA-binding protein ProQ, that interact with sRNA – target RNA complexes. The general experimental procedure involves the cross-linking of the RBP-sRNA/target RNA complex followed by immunoprecipitation and sequencing of the purified RNA molecules (Saliba *et al.*, 2017). However, in the *H. pylori* genome, neither Hfq nor ProQ orthologues are represented, thus limiting the available techniques for regulatory RNAs and/or sRNAs interactors identification (Tejada-Arranz *et al.*, 2021).

To overcome this limitation, in recent years a tagging approach called MS2-affinity purification coupled with RNA sequencing (MAPS) was developed to identify direct sRNAs interactors *in vivo*. This technique exploits the strong affinity of the capsid protein of the MS2 bacteriophage for the short 43 nt MS2 RNA aptamer used to tag the sRNA of interest. After the expression *in vivo* of the MS2-tagged sRNA, cell lysates are incubated with an amylose resin carrying a maltose binding protein fused with MS2 protein (MBP-MS2 protein). Bound RNA is eluted with a maltose-supplemented buffer, and the purified affinity chromatography product containing the MS2-tagged sRNA complexed with its RNA interactors is then sequenced (Carrier *et al.*,2016).

The MAPS approach has been successfully employed in the Gram-negative bacterium *E. coli* to uncover the interactome of the three well-characterized sRNAs RyhB, RybB and DsrA, revealing previously unknown targets (Lalaouna *et al.*, 2015a; Lalaouna *et al.*, 2015b;). Further, methodologies based on MS2-affinity purification (i.e., coupled with mass spectrometry) have been proposed to reveal promising protein partners as RNA binding proteins or ribonucleases associated with sRNA, enlarging the potential of the MAP-based platform (Rieder *et al.*, 2012; Lalaouna *et al.*, 2017).

We implemented the MS2-affinity purification approach in the *H. pylori* G27 strain to identify new potential targets of the sRNA CncR1. We validated the system by comparing the

expression of the MS2-tagged and untagged *cncR1* sRNA in different strains. In addition, a preliminary analysis of the affinity chromatography is reported, demonstrating the suitability of the MAPS approach in this strain.

3.2.2 Construction of MS2-tagged and untagged isogenic cncR1 mutants

The first step to apply the MS2-affinity purification to determine CncR1 interactome consisted in the generation of the *cncR1* knockout mutant (Δ*cncR1*). To this purpose, *H. pylori* G27 wild type strain was transformed with the double-joint PCR product *cncR1*-UP::CpR::*cncR1*-DOWN in which most of the *cncR1* sequence and 65 bp of the P_{cagP} promoter were replaced by the chloramphenicol resistance cassette. Then, starting from Δ*cncR1* genetic background, we generated Δ*cncR1*::*cncR1* and Δ*cncR1*::MS2-*cncR1* complemented strains, harbouring the wild type *cncR1*-S and 5'- MS2-tagged *cncR1*-S sequences, respectively, under the control of the native P_{cagP} promoter and cloned in the *vacA* locus. As a control, starting from the Δ*cncR1* strain we generated a mutant harbouring the MS2 aptamer sequence directly fused with the *cncR1-S* terminator and cloned in the *vacA* locus under the control of P_{cagP} promoter (Δ*cncR1*::MS2-term). Mutants were confirmed by sequencing of the genomic regions of interest.

To evaluate the correct *cncR1* expression and stability, primer extension analyses were performed on RNAs extracted from liquid cultures of Δ*cncR1*, Δ*cncR1*::*cncR1*, Δ*cncR1*::MS2-*cncR1* strains and the parental wild type strain. Since *cncR1* levels significantly decreased at the beginning of the stationary phase (Vannini *et al.*, 2016), bacterial cells were harvested at mid-exponential phase of growth (OD_{600} = 0.6-0.7). In addition, a Sanger sequencing experiment allowed the mapping of the *cncR1* TSS in the different mutants. While *cncR1* transcript was entirely lost in the Δ*cncR1* strain, the Δ*cncR1*::*cncR1* and Δ*cncR1*::MS2-*cncR1* complemented strains restored *cncR1* expression to wild type levels (Fig. 10). Importantly, a 43 nt increase in size of *cncR1*-MS2 transcript was detected in Δ*cncR1*::MS2-*cncR1* strain compared to the wild type and Δ*cncR1*::*cncR1* strains, and corresponded to the MS2 aptamer. These results indicated that the MS2 aptamer fused to the *cncR1* 5'-end did not affect its expression or stability.

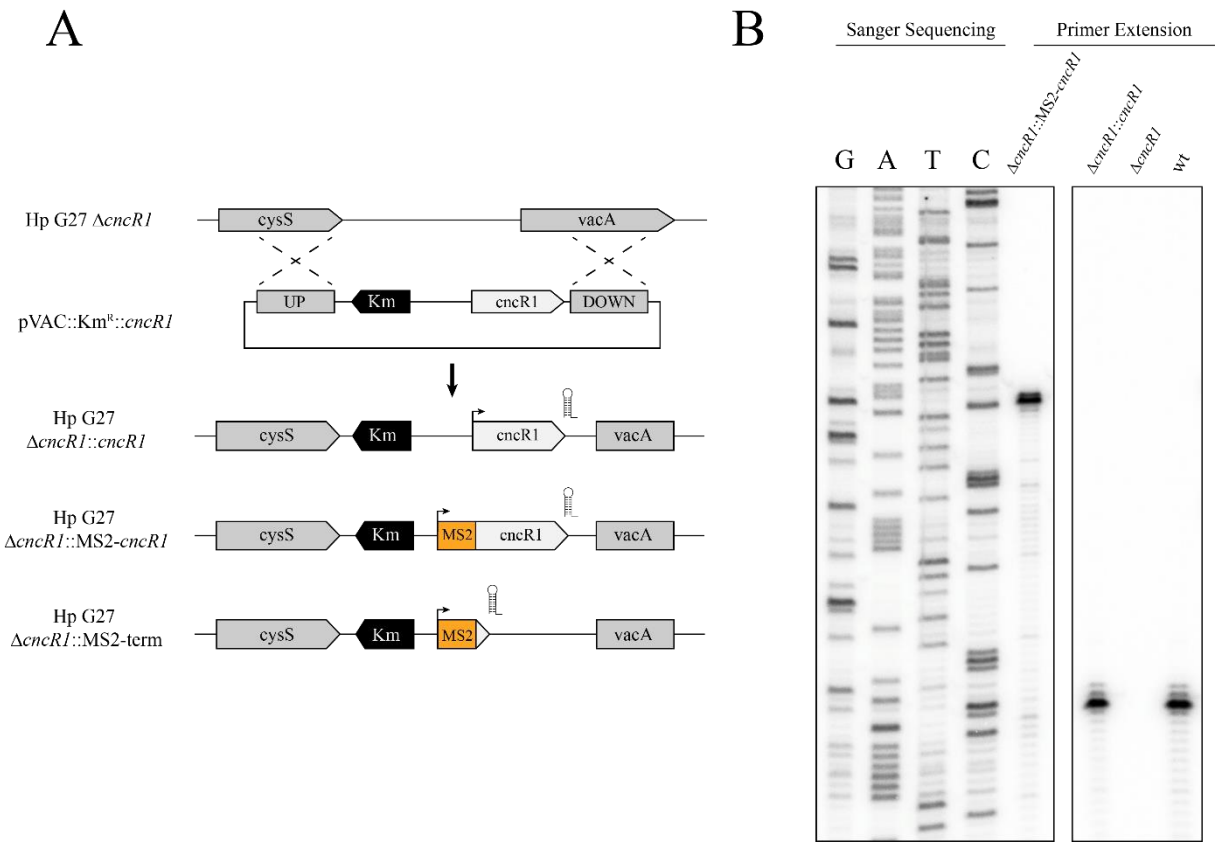

Figure 10: **A**) Schematic representation of the procedure employed to obtain the Δ*cncR1*::*cncR1*, Δ*cncR1*::MS2-*cncR1*, and Δ*cncR1*::MS2-term strains. The pVAC::Km::*cncR1* vector carrying the 539 bp "UP" region of homology with *cysS* (HP0886), the 745 bp "DOWN" region of homology with *vacA* (HP0887), the Km^R cassette and a 427 bp fragment encompassing P_{cagP} promoter and *cncR1-S* gene, was used to transform the G27 Δ*cncR1* mutant to obtain Δ*cncR1*::*cncR1* complemented strain. Vectors pVAC::Km^R::MS2-*cncR1* and pVAC::Km^R::MS2-term, harbouring 5'- MS2-tagged *cncR1* and the MS2 tag alone respectively, were used to obtain Δ*cncR1*::MS2-*cncR1* and Δ*cncR1*::MS2-term strains. **B**) Primer extension performed with the radioactively labelled 536pe17 probe on total RNA extracted from the wild type, Δ*cncR1*, Δ*cncR1*::*cncR1*, and Δ*cncR1*::MS2-*cncR1* strains. Sanger sequencing performed on pVAC::Km^R::MS2-*cncR1* allowed to map the correct insertion of MS2.

3.2.3 Preliminary analysis of MS2-affinity chromatography samples

To identify *in vivo* complexes involving CncR1 sRNA and its target RNAs, we adopted the MS2-affinity purification approach. Briefly, Δ*cncR1*::MS2-*cncR1* strain, expressing MS2-tagged *cncR1*, and the two Δ*cncR1*::*cncR1* and Δ*cncR1*::MS2-term control strains, expressing un-tagged CncR1 and the MS2-tag alone, respectively, were grown to mid-exponential growth phase (OD_{600} = 0.6-0.7). Cells were then lysed in a French Press cell disruptor and total extract was subjected to affinity chromatography as described in Materials and Methods. After elution, the RNA was extracted, the contaminating DNA was depleted by enzymatic digestion and the resulting samples were converted to cDNAs and analysed by RT-qPCR to check the relative enrichments of the different RNA species.

MS2-*cncR1* enrichment by MS2 capture was calculated measuring the *cncR1* transcript levels in samples obtained from Δ*cncR1*::MS2-*cncR1* strain with respect to the Δ*cncR1*::*cncR1* strain. As shown in Fig. 11, after the affinity chromatography, MS2-*cncR1* was strongly enriched (110-fold change) compared to *cncR1* alone, because of the capture by MBP-MS2 fusion protein. The same procedure performed on Δ*cncR1*::MS2-term strain, which is knock-out for *cncR1*, showed non-specific background noise for *cncR1*.

For the target analysis, to exclude non-specific enrichments by MBP-MS2 capture, the enrichment of putative targets was measured by comparing their levels in the MS2-*cncR1* sample after purification with respect to those in the MS2-tag alone, which was set as the reference of the experiment. In Fig. 11 are reported the most representative genes selected among all those analysed.

FliK, which was previously reported to interact *in vivo* and *in vitro* with CncR1 in correspondence of multiple sequences along its CDS (Vannini *et al.*, 2016), did not result enriched in the MS2-*cncR1* purification sample. In contrast, mRNAs of *hrcA*, encoding for an important transcription repressor induced by heat shock stress, and of *pfr*, encoding for the iron storage ferritin, showed an enrichment of 2.1-fold and 3.2-fold, respectively. Noteworthy, *hrcA* was proposed to belong to the CncR1 regulon, as its transcript level is reduced when CncR1 sRNA is deleted (Vannini *et al*., 2016).

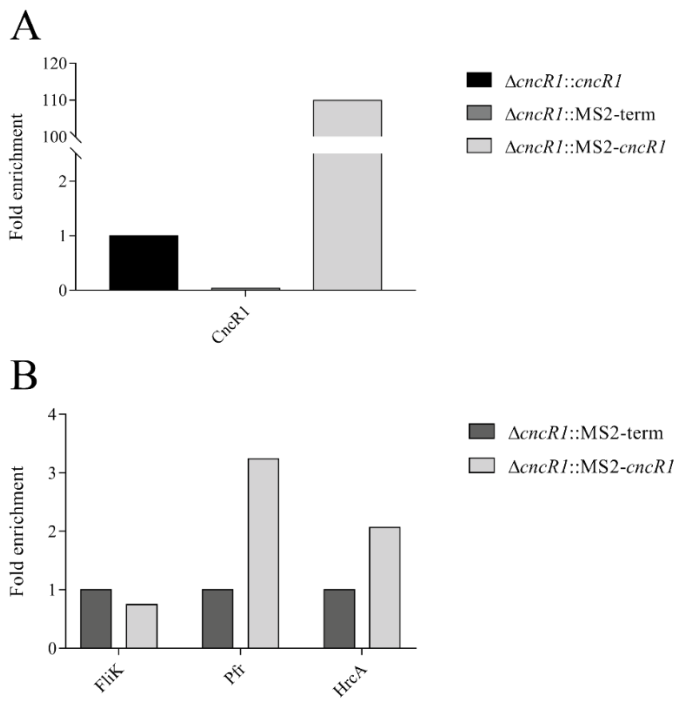

Figure 11: RT-qPCR analysis of MS2-affinity chromatography experiments performed on Δ*cncR1*:: *cncR1*, Δ*cncR1*::MS2-*cncR1* and Δ*cncR1*::MS2-term strains. A) Fold enrichment values of *cncR1* transcript were calculated subtracting the Ct values of the *cncR1*-alone control sample from the other Ct values. B) Fold enrichment values of the tested genes were calculated with the ΔΔCt method. Briefly, ΔCt was calculated for each gene by subtracting the Ct values of the MS2-tag alone control sample from the MS2-*cncR1* Ct values. A ΔCt mean value was calculated considering all the genes tested in the RT-qPCR assay (i.e. *fliK*, *flab*, *flgE*, *flgB* and *dppF*) and ΔΔCt values were calculated subtracting the calculated ΔCt mean value from the ΔCt of each gene.

4. Discussion

The capacity of the human pathogen *H. pylori* to adapt to the restricted host-associated environment (i.e., the gastric niche) and to evade the host immune response largely depends on its streamlined and efficient signalling network (Mo *et al.*, 2022). Regardless of the lack of transcriptional regulators, in the last few years, several studies pinpointed the potential offered by the asRNA and sRNA in the post-transcriptional orchestration of gene expression in response to stress conditions such as oxidative stress, acid pH, nickel starvation and antibiotics (Pernitzsch *et al.,* 2012; Tejada-Arranz and De Reuse 2021). In addition, their deletion or improper expression often led to severe phenotypes showing an increased susceptibility to antibiotics, hampered motility and reduced adhesion to host cells (Eisenbart *et al.,* 2020). In this perspective, the control over the decay and maturation of different RNA classes is of primary importance to ensure the maintenance of cellular homeostasis. Recent studies regarding the RNA degrading machinery in *H. pylori* highlighted the role of RNase J, as the primary participant in the initiation of bulk mRNA and asRNAs decay, and RNase III and RNase R, as involved to different extents in the maturation of stable rRNAs (Redko *et al.,* 2016; Iost *et al.,* 2019; Tejada-Arranz *et al.,* 2021). However, the mechanisms regarding the degradation and maturation of the sRNAs in *H. pylori* remain almost unknown.

With the primary aim of unveiling a master regulator involved in sRNAs metabolism, in this study we provide for the first time a functional characterisation of the single-strand specific endo-RNase Y in *H. pylori* G27.

The RNase Y in *H. pylori* G27 is encoded from the *rny* gene. In accordance with the polycistronic organisation observed for the compact genome of the 26695 strain (Sharma *et al.,* 2010), our analysis of the *rny* genomic locus revealed that this gene is transcribed in tandem with HP0761 from the P_{761} promoter. The nucleotide sequence of the P_{761} promoter indicates a conserved -10 TATAAT box recognised by the vegetative σ^{80} factor of the RNA polymerase, without nor extended TGn element, neither a -35 box (Fig 1B). In accordance with the presence of an apo-Fur-like TCATT-n12-TT consensus sequence, the homo-dimeric apo-Fur protein was capable of binding in vitro within the P_{761} promoter even at the lowest tested iron concentration (Fig. 2A). Further, our transcriptional studies showed that in iron-depleted conditions, the *rny* gene is overexpressed in a wild type strain and that such regulation is partially lost in a strain mutated for the Fur regulator. These results suggest that the intracellular levels of the *rny* transcript could be regulated as a function of both iron concentration and Fur presence. Curiously, both in Fe^{2+}-depleted and Fe^{2+}-repleted conditions, the pleiotropic Fur regulator has mainly been described as a transcriptional repressor (Bereswill *et al*., 2000; Delany *et al*.,

2001b; Delany *et al*., 2002b). The *rny* gene could represent the first-ever described case of a positive induction mediated by apo-Fur.

Studying the aminoacid sequence of RNase Y, we observed that the domains and motifs required for the proper activity of this enzyme in other bacteria, such as *B. subtilis*, are conserved in *H. pylori*. We found that the transcription levels of virtually all genes, including *fliK*, *flaB*, *flgE* and *cncR1*, expressed in the mutant coding for an RNase Y carrying a His-Ala substitution in the predicted catalytical site (*Δrny::rny*^{H374A}) resembled the transcription levels of a knock-out mutant. This suggests the crucial role of the His residue in the phosphohydrolitic activity of the RNase Y. Similar results were observed in *B. subtilis*, where mutations in the metal-chelating HD domain hampered the RNase Y's ability to process a riboswitch located in the *yitJ* leader region (Shababian *et al.,* 2009). Consistent with previous evidences that proteins involved in RNA degradation are sometimes negatively autoregulated through the stability of their own mRNAs (Jain and Belasco, 1995; Robert-Le Meur and Portier, 1994; Deutscher, 2015), we observed a significant increase in the *rny* transcript levels in *Δrny::rny*^{H374A} mutant. Indeed, in a model in which a functional RNase Y enzyme is subjected to a potent autoregulation mechanism, the expression of an inactive enzyme likely results in the accumulation of its own transcript.

The compartmentalisation of the degrading machinery is typical and has been speculated to reflect the turnover of specific subcategories of genes (Tejada-Arranz *et al.,* 2020). In accordance with the presence of an N-terminal transmembrane domain, we localised the RNase Y at the cell's periphery. However, its presence in the outer membrane fraction remains controversial and needs further investigation. Although Voss and co-workers excluded the RNase Y during their comprehensive characterisation of *H. pylori* outer membrane proteins, this protein was enriched in the insoluble fraction following a fractionation protocol performed with Triton X-100 gradient (Voss *et al.,* 2014). Considering the lack of positive control for the inner membrane fraction in our experiment, it is conceivable that the RNase Y may be a highly insoluble protein and prone to spontaneous self-aggregation in the tested conditions. In addition, as we deleted the 26 residues corresponding to the transmembrane domain, we were unable to detect the protein in any of the fractions, nor in the total extract (Fig 5), suggesting that protein truncation may lead to an incorrect folding of the protein followed by degradation phenomena.

In contrast to the RNase J, which is essential for the viability of the cell (Redko *et al.,* 2013), the deletion or inactivation of the RNase Y has a moderate impact on the *H. pylori* fitness, causing only a 30% retardation on *H. pylori* doubling time. In addition, as revealed from the transcriptome analysis, the deletion of the RNase Y triggered changes in the transcript levels of

only a small number of 68 genes. The small RNase Y regulon is consistent with the fact that RNase Y is not essential under standard growth conditions. Such a modest influence on global transcript levels upon RNase Y depletion has already been documented in *S. pyogenes*, where this enzyme is not essential and is primarily responsible for the stabilisation of transcripts (Bugrysheva *et al.,* 2010 Chen *et al.,* 2013; Broglia *et al.,* 2020). From our analysis, overall, several genes encoding virulence factors involved in gastric environment adaptation (*ureB*) host-pathogen interaction (*sabA*, *hopA*, horL, *alpA*, *alpB* and *hopQ*), motility (*flaB*, *fgE* and *fliK*) and chaperones (*groEL*) were up-regulated. Intriguingly CncR1 is the only trans-acting sRNA with regulatory function represented in our transcriptome analysis. The presence of this transcript among the up-regulated genes contrasts with the overexpression of motility genes, as it was shown to negatively correlate with genes involved in flagellar assembly and biogenesis (Vannini *et al.,* 2106). This observation, in addition to the involvement of RNase Y in the maturation and processing of different RNA molecules in other pathogens (Shababian *et al*., 2009; DeLoughery *et al.,* 2018), prompted us to investigate this phenomenon.

This project's second line of research aimed at characterising the Rnase Y activity on the trans-acting sRNAs represented in *H. pylori*. Vannini and collaborators characterised for the first time CncR1 as a 213 bp sRNA arising from the P_{cagP} promoter and whose transcription is phase-of-growth controlled by the master regulator HP1043 (Vannini *et al.,* 2016). We demonstrate that when the RNase Y is depleted or inactivated, a secondary transcript arising from the same CncR1 locus accumulates in the cell. Taking advantage of RNAfold bioinformatic tool and Northern blot experiments performed on the 3' region downstream of the known CncR1 terminator, we revealed that this secondary transcript (which we called CncR1-L) terminates at a secondary strong (-40.16 KJ/mol) terminator sequence located ~320 bp after the CncR1 transcription start site. Although the presence of an alternative transcript (CncR1-L) from the P_{cagP} promoter has already been proved in wild type conditions, it was considered a barely detectable readthrough or unprocessed product (Vannini *et al.,* 2016). Our data further show that in the absence of a functional RNase Y enzyme, the stability of only CncR1-L is increased, but not that of CncR1. These evidences allowed us to speculate a model in which the RNase Y acts in order to degrade the CncR1-L readthrough product or to process the CncR1-L to obtain a mature CncR1 molecule. The hypothesis of CncR1-L as an immature precursor would agree with the increased expression of flagellar genes observed in both *ΔcncR1* and *Δrny* strains (Vannini *et al.,* 2016). Indeed, a single-strand endo-RNase processing step is frequently needed for maturation of IGRs encoded sRNAs to reveal the seed region, increase their stability, or even produce two independent sRNA molecules with different regulons (Svensson and Sharma., 2021; Saramago *et al.,* 2014). Unfortunately, similar results were not obtained neither

for RepG nor for NikS (data not shown) sRNAs as their transcripts remained stable even in the absence of RNase Y. This suggests that the RNase Y activity could be strictly related to CncR1-L in a sequence- or structure-specific manner.

In the last part of this project, we focused on the research of direct interactors of CncR1 through MAPS technology. Our knowledge about the regulon of CncR1 is based "solely" on transcriptome analysis of a CncR1 knock-out strain and in vitro experiments which identified the *fliK* transcript as the only direct target of the sRNA. Intriguingly, our preliminary results suggest *pfr* and *hrcA* as possible direct CncR1 interactors in vivo, but not *fliK*. In particular, the *hrcA* gene encodes for the pleiotropic heat-shock transcriptional repressor HrcA, which is known to be implicated in the transcriptional regulation of a plethora of genes involved in motility, Ni^{2+} trafficking, hot-pathogen interaction, LPS biosynthesis and others (Roncarati *et al.*, 2019). The observation that CncR1 could interact and thus coordinate the post-transcriptional regulation of *hrcA*, further underlines the importance of this sRNA in *H. pylori* virulence. However, even considering all the limits related to this preliminary approach (i.e., the analysis of specific targets by RT-qPCR instead of a more comprehensive RNA-seq), we pose the basis for further in-depth studies, which will hopefully unveil the interactome of CncR1.

5. Materials and Methods

5.1 Bacterial Strains and growth conditions

All the *H. pylori* strains employed are listed in Table 1. Bacteria were recovered form -80°C glycerol stocks (Brucella broth + 20% glycerol) and plated onto Brucella agar (BA) plates containing 7.5% fetal calf serum supplemented with Dent's antibiotic supplement, unless otrherwise stated. Bacteria were grown for 24-48 hours at 37°C in jars using CampyGen™ (Thermo Fisher) atmosphere generation systems or in a water-jacketed thermal incubator (9% CO_2, 91% air atmosphere, and 95% humidity). Liquid cultures were grown in Brucella broth (BB) medium supplemented with 7.5% inactivated fetal calf serum (FCS) and Dent's antibiotic supplement at 37°C with gentle agitation (140 rpm), in glass flasks until the indicated growth phase was reached. For transformant selection and growth of mutant strains, chloramphenicol (30 μg /ml) and kanamycin (25 μg/ml) were added to solid media. For iron treatment, late exponential phase bacterial cultures (OD_{600}=1.0.-1.1) were exposed for 20 min to freshly prepared 1 mM $(NH_4)_2Fe(SO_4)_2$ or 150 μM 2,2′-Dipyridyl.
E. coli strains DH5α and BL21 (DE3) cultures were grown in Luria-Bertani (LB) agar or in LB broth. When required, ampicillin, kanamycin and chloramphenicol were added at final concentration of 100 μg/ml, 25 μg/ml, and 30 μg/ml, respectively.

Table 1: Strains used in this study.

Strain	Genotype or Description	Source
***E. coli* strains**		
DH5α	supE44 ΔlacU169 (ϕ80 lacZΔM15) hsdR17 recA1 endA1 gyrA96 thi-1 relA1β	(Hanahan, 1983)
BL21 (DE3)	F^- ompT hsdSB (rB^-, mB^-) gal dcm (DE3)	Invitrogen
***H. pylori* strains**		
G27	Clinical isolate; wild-type parental strain	(Xiang *et al.*, 1995)
Δ*fur*	G27 derivative; bp 25 to 434 of the *fur* (HP1027) coding sequence replaced by a *km* cassette; Km^R	(Delany *et al.*, 2001a)
Δ*rny*	G27 derivative; bp from 135 to 1487 of the *rny* (HP0760) coding sequence were replaced by a *km* cassette: Km^R	This study
Δ*rny*::*rny*	G27 Δ*rny* derivative; contain HP0761, *rny* and the upstream P_{761} promoter cloned in the *vacA* locus. HP0761 harbours an in-frame deletion from bp 26 to 519 of its CDS. Km^R, Cp^R	This study
Δ*rny*::rny^{H374A}	G27 Δ*rny* derivative; contain HP0761, *rny* and the upstream P_{761} promoter cloned in the *vacA* locus. *Rny* harbours an H374A mutation. HP0761 harbours an in-frame deletion from bp 26 to 519 of its CDS. Km^R, Cp^R	This study

Δ*rny*::*rny*-FLAG	G27 Δ*rny* derivative; contain HP0761, *rny*-1xFLAG fusion and the upstream P_{761} promoter cloned in the *vacA* locus. HP0761 harbours an in-frame deletion from bp 26 to 519 of its CDS. Km^R, Cp^R	This study
Δ*rny*::*rny*$^{\Delta TMh}$-FLAG	G27 Δ*rny* derivative; contain HP0761, *rny*-1xFLAG fusion and the upstream P_{761} promoter cloned in the *vacA* locus. *Rny* harbours a deletion for the first 78 bp of its CDS. HP0761 harbours an in-frame deletion from bp 26 to 519 of its CDS. Km^R, Cp^R	This study
Δ*cncR1*	G27 derivative; bp from -65 to 195 of the *cncR1* (HP0536 5' UTR) sequence were replaced by a *cat* cassette: Cp^R	This study
Δ*cncR1*::*cncR1*	G27 Δ*cncR1* derivative; sequence from position -170 to 257 of *cncR1* is cloned in the *vacA* locus; Cp^R, Km^R	This study
Δ*cncR1*::MS2-*cncR1*	G27 Δ*cncR1* derivative; contain 5' MS2-tagged *cncR1* and the upstream PcagP promoter cloned in the *vacA* locus: Cp^R, Km^R	This study
Δ*cncR1*::MS2-term	G27 Δ*cncR1* derivative; contain MS2-tag fused to *cncR1* terminator and the upstream PcagP promoter cloned in the *vacA* locus: Cp^R, Km^R	This study

Table 2: Plasmids and constructs used in this study.

Name	**Description**	**Source**
Plasmids		
pBluescript KS II+	Cloning vector, Ap^R	Stratagene
pBS::*cat*	pBluescript KS II derivative carrying a HincII *Campylobacter coli cat* cassette from pDT2548 (Wang and Taylor, 1990) cloned into the SmaI site of the vector; Ap^R, Cp^R	Vannini *et al.*, 2012
pNKO::Km^R	Suicide vector; Ap^R, Km^R	Pflock *et al.*,2005
pHMM	Plasmid expressing the His-tagged MBP-MS2 capsid fusion protein; Ap^R, Km^R	Batey and Kieft, 2007
pVAC::Km^R	pGEM3Z derivative containing the C. coli aphA-3 cassette flanked by upstream and downstream regions for double homologous recombination in the vac locus; Ap^R, Km^R	Delany *et al.*, 2002
pVAC::CAT	pVAC::Km derivative, carrying a BglII/BamHI cat cassette from pBS::cat; Ap^R, Cp^R	Pepe *et al.*, 2018
pVAC::Km-*cncR1*	pVac::Km^R derivative, containing a 416 NcoI/SalI fragment amplified with oligo CncR1F-NcoI and CncR1R-SalI on H. pylori G27 chromosomal DNA; Ap^R, Km^R	This study

pVAC::Km-MS2-*cncR1*	pVac::Km^R derivative, harbouring a 281 bp Nco-blunt fragment amplified with oligos CncR1F-Nco and MS2a-R and a 182 bp blunt-SalI fragment amplified with oligos MS2-F and CncR1R-SalI. Both the fragments were amplified from H. pylori G27 chromosomal DNA; Ap^R, Km^R	This study
pVAC::Km-MS2-term	pVAC::Km::MS2-cncR1 derivative obtained by whole around PCR with oligos cncR1_term-wa_F and MS2-wa_R harbouring the MS2 sequence upstream the terminator of CncR1-S sequence. Ap^R, Km^R	This study
pVAC::CAT-P$_{761}$-HP0761-*rny*	pVAC::CAT derivative containing a 2518 bp XbaI/KpnI fragment amplified with oligos 716-F_XbaI and 717-R_KpnI on the H. pylori G27 chromosomal DNA; Ap^R, Cp^R	This study
pVAC::CAT-P$_{761}$-*rny*	pVAC::CAT::761-rny derivative obtained by whole around PCR with oligos Δ717wa_F and Δ717wa_R . HP0761 harbours an in-frame deletion from bp 26 to 519 of its CDS; Ap^R, Cp^R	This study
pVAC::CAT-P$_{761}$-*rny*^{H374A}	pVAC::CAT::*rny* derivative obtained by mutageneis PCR with oligos YH374A-F and YH374A-R; Ap, Cp^R	This study
pVAC::CAT-P$_{761}$-*rny*-FLAG	pVAC::CAT::*rny* derivative obtained by whole around PCR with oligos Y_C-FLAG_Fw and Y_C-FLAG_Rev and carrying a 1xFLAG epitope fused to the rny gene	This study
pVAC::CAT-P$_{761}$-*rny*^{ΔTMh}-FLAG	pVAC::CAT::*rny*-FLAG derivative obtained by whole around PCR with oligos ΔTMh_Fw and ΔTMh_Rev	This study
Constructs		
cncR1_UP-Cp^R-cncR1_DOWN	Double-joint PCR construct carrying a 614 bp region amplified on H. pylori G27 chromosomal DNA with oligos cncR1-UPdj-F and cncR1-UPdj-R2, a 792bp *cat* cassette amplified from a pBS::*cat* vector with the oligos CAT-dj-F and CAT-dj-R, and a 465 bp region amplified on H. pylori G27 chromosomal DNA with oligos cncR1-DOWNdj-F and cncR1-DOWNdj-R; Cp^R	This study
rny_UP-Km^R-rny_DOWN	Double-joint PCR construct carrying a 520 bp region amplified on H. pylori G27 chromosomal DNA with oligos YKO-up-F and YKO-up-R-T, a 792 bp *aphA3* cassette amplified from a pNKO::Km^R vector with the oligos KmF and KmR, and a 573 bp region amplified on H. pylori G27 chromosomal DNA with oligos YKO-down-F-T and YKO-down-R; Km^R	This study

Table 3: Oligonucletides used in this study.

Oligonucletides	Sequence	Source
cncR1-UPdj-F	CCATATCAAAAACAAATTACTAACACACTA	This study
cncR1-UPdj-R2	CGCACTTCTATACTCTCTGTCGGCCCTGAACTACTTCTTTAAAAAC	This study
CAT-dj-F	AACCGTGATATAGATTGAAAAGTGG	This study
CAT-dj-R	CGACAGAGAGTATAGAAGTGCG	This study
cncR1-DOWNdj-F	CCACTTTTCAATCTATATCACGGTTAGAAAAACATAACACTATAAGACCTG	This study
cncR1-DOWNdj-R	CCATAAGCCTTTGACTTAGCAGTAAGG	This study
YKO-up-F	ATCGCCACAGAATATGCGCATTTG	This study
YKO-up-R-T	CTAGATTTAGATGTCTAAAAAGCTTATCGATCGCTAAAAAGATAGAAGAGAGTGC	This study
KmF	ATCGATAAACCCAGCGAACCATTTG	This study
KmR	TCGATAAGCTTTTTAGACATCTAAATCTAG	This study
YKO-down-F-T	CCTCAAATGGTTCGCTGGGTTTATCGATTAGCTGAAGCACTTTTTAAAGTAGC	This study
YKO-down-R	TTAGGGCATGAGCTTGACATTAG	This study
CncR1F-NcoI	AGTTCCATGGTTTTAATTTGCTAATTTGGT	This study
CncR1R-SalI	CAAAGTCGACCAATACATTTTACCACAATT	This study
MS2a-R	GTTTTTCAGACACCATCAGGGTCTGGTGTT	This study
MS2-F	GTACCCTGATGGTGTACGAAATCCATTATA	This study
cncR1_term-wa_F	GCTCCTTTGTAAGTTCACCGCCC	This study
MS2-wa_R	CAGACCCTGATGGTGTCTGAAAAACG	This study
716-F_XbaI	TATATCTAGAGGATCATGCCCATTTACTTGC	This study
717-R_KpnI	TATAGGTACCGTGGTATTGTTTTGAGAATCTTGAG	This study
Δ717wa_F	GCAAGCCAATTTATCCCTGAC	This study
Δ717wa_R	CTTTACATGAATGCTCGTATCGTTATG	This study
YH374A-F	CCGGTATTTTGGCTGATATTGGTAAAGCGC	This study
YH374A-R	CTCTTCTGGCGAGCTTTTTATCC	This study
Y_C-FLAG_Rev2	GATGATAAATAATCAAGCTTTTTTCCCGCACC	This study
Y_C-FLAG_Fw	ATCATCTTTATAATCTTGCTTGAGCGTAGCGG	This study
ΔTMh-Fw	AATGTTTCCTCTTATTATTCTTCATAACG	This study
ΔTMh-Rev	ATGAAAAAGATCTATTACGCTAGAGGG	This study
716-F	AAGCCATGTAATTGAGCATCG	This study
717-R	GAGCCGAGTTTATCGCACC	This study
717-F	GCAAGCCAATTTATCCCTGAC	This study
718-R	TTAGGGCTATCTTGTTGGGTGG	This study
AD_HP0761_RTF	TGCAAGCCAATTTATCCCTGAC	This study
AD_HP0761_RTR	AGAGATTTTTGTAAAGAACGCTTGA	This study
16S-RTF	GGAGTACGGTCGCAAGATTAAA	Vannini *et al.*, 2016
16S-RTR	CTAGCGGATTCTCTCAATGTCAA	Vannini *et al.*, 2016

RNaseY_RTF	TCTATATCCACCCCGCTGAC	This study
RNaseY_RTR	GTCGTGTGATAGGCAAAGACG	This study
536-RTF	AGGGCGGTGAACTTACAAAG	Vannini *et al.*, 2016
536-RTR	CGTTTTTCAGACACCATCAGG	Vannini *et al.*, 2016
NikS-RTF	GCGAAAGGCGTATTATATTCCTTCCTTC	This study
NikS-RTR	GGGGAAAGGTAAGAGCGTCAGG	This study
RepG-RTF	CAAGACAAAGGGAAAGGAGGGG	This study
RepG-RTR	CATTCCTTATGGTTTGGTTGGCAC	This study
Flik5-RTF	CCCTAAAAGATTTGCTCAACCAC	This study
FliK5-RTR	CTCCATTAGGCTCTTTTTCATTCTTG	This study
115RTF	ACCGCAGATAAAGCGATGGA	Vannini *et al.*, 2016
115RTR	GAGCGCTCTTCGGCTTTCTA	Vannini *et al.*, 2016
870RTF	GATGCAAGCCCACCAAATCG	Vannini *et al.*, 2016
870RTR	GCGCAGTAGCGATGAGTTTG	Vannini *et al.*, 2016
1559-RTF	AGGCGTTGGATTATCGGTCTT	Vannini *et al.*, 2016
1559_RTR	TTTGGCCTGTAAAAGGGGGT	Vannini *et al.*, 2016
pfrRT-fwd	TGCTGTTCAGCCACATACCATTGC	Roncarati *et al.*, 2019
pfrRT-rev	GCGCCTGAGCATAAGTTTGAAGGT	Roncarati *et al.*, 2019
hrcRT_fw	AGGGCGTGTTACTAGCATGCAATC	Roncarati *et al.*, 2019
hrcRT-rev	GGCCAGACAATTAGAGCGTTTGGA	Roncarati *et al.*, 2019
536pe17	AACGATTTGTTTGTTTATGC	Vannini *et al.*, 2016
536pe20	TTTGCTAATTTGGTTGTTCC	Vannini *et al.*, 2016
5S-F	CGACCTACATTCCCACTCTTG	This study
5S-R	CCGAACCTGGAAGTCAAGC	This study

5.2 Construction of *Helicobacter pylori* mutant strains

H. pylori mutants were obtained by double homologous recombination of the naturally competent G27 strain as previously described (Chevalier *et al.,* 1999). Briefly, *H. pylori* was recovered from working stock and restreaked two times in fresh BA plates. Freshly grown cells were then streaked in small circles in fresh BA plates and grown for further 3-4 hours to stimulate the natural competence. For transformation, 8 μg of plasmid DNA or 2 μg of purified PCR product were added onto the growing cells. After an overnight incubation, trasformants were selected on BA plates supplemented with chloramphenicol or kanamycin, according to the resistance phenotype conferred by the *Campylobacter coli cat* (Cp^R) and *aphA3* (Km^R) cassettes, respectively. Mutants were observed after 3-7 days of incubation All *H. pylori* mutants were checked for correct transformation by PCR and/or sequencing of isolated gDNA.

5.3 Construction of isogenic Δ*cncR1* mutant strain

The *H. pylori* Δ*cncR1* mutant strain, carrying a knock-out deletion for the *cncR1* sRNA (corresponding to the annotated 5'UTR of HP0536), was obtained by double homologous recombination of a G27 wild type strain using a cncR1_UP-Cp^R-cncR1_DOWN amplicon that was constructed with a Double-joint PCR as described in Yu *et al.,* 2004. Briefly, the 614 bp up- and the 465 bp down-stream homologous regions were amplified from Hp G27 WT gDNA using the primers cncR1-UPdj-F/cncR1-UPdj-R2 and cncR1-DOWNdj-F/cncR1-DOWNdj-R respectively. *Campylobacter coli cat* chloramphenicol resistance cassette (792bp) was amplified from a pBS::*cat* vector with the oligos CAT-dj-F/CAT-dj-R. The PCR products were then mixed in a 1:3:1 (UP:cat:DOWN) ratio in a second PCR reaction and cycled for few times, to allow the extension and fusion of the three products. Finally, a third PCR reaction performed using cncR1-UPdj_F/cncR1-DOWNdj-R primers, allowed the amplification of the resulting product of 1871 bp. 2 μg of the purified amplicon were then used to transform *H. pylori*. Transformants were selected on BA plates containing 30 μg/ml chloramphenicol and mutants were checked by sequencing the isolated gDNA.

5.4 Generation of the complemented Δ*cncR1* mutant strains

To complement the G27 *cncR1* knock-out (Δ*cncR1*) strain with *cncR1* wild type or MS2-tagged sequences, we selected the *vacA* gene locus, as it was routinely used in our laboratory for the ectopic complementation of different genes. Vector pVAC::Km^R-cncR1 was used to generate the complemented Hp G27 Δ*cncR1*::*cncR1* strain and it was designed as follows. A 416 bp fragment encompassing the *cncR1* sRNA and its own promoter sequence was amplified from genomic DNA of Hp G27 WT strain with oligonucleotides CncR1F-NcoI and CncR1R-SalI and NcoI/SalI inserted in the pVAC::Km^R vector. This vector harbours the *aphA-3* gene, which confers resistance to kanamycin, flanked by a 529 bp homologous regions to *cysC* gene and a 752 bp homologous region to vacA gene (Delany *et al.,* 2002).

To generate the MS2-tagged complemented Hp G27 Δ*cncR1*::MS2-*cncR1* strain a pVAC::Km^R-MS2-cncR1 plasmid was constructed. A 281 bp NcoI-blunt fragment harbouring the whole cncR1-encoding region linked to half (25 bp) of MS2 tag sequence, and a 182 bp blunt-SalI fragment encompassing the other 18 bp of MS2 tag sequence in attrition to the cncR1 promoter region, were amplified from genomic DNA of Hp G27 WT strain and NcoI/SalI cloned into pVAC::Km^R vector.

pVAC::Km^R-MS2-term plasmid was constructed to generate the control strain Hp G27 Δ*cncR1*::MS2-term. Exploiting a whole around PCR with oligos cncR1_term-wa_F and MS2-

wa_R on a pVAC::Km^R-MS2-cncR1 template the *cncR1* sRNA core sequence was deleted and the MS2 tag was blunt-ligated to the last 37 bp of *cncR1* corresponding to its terminator.
To avoid polar effects and to transcriptional readthrough, all *cncR1* constructs were cloned in a divergent orientation compared to *aphA-3* gene. All recombinant vectors were checked by colony PCR. After *H. pylori* transformation (as described above), complemented Hp G27 strains were checked by gDNA sequencing of the *vacA* recombinant locus.

5.5 Construction of isogenic Δ*rny* mutant strain

H. pylori mutant carrying the deletion for the *rny* gene (HP0760) was realized by double homologous recombination of a G27 wild type strain using a rny_UP-Km^R-rny_DOWN amplicon constructed with a Double-joint PCR as described in Yu *et al.*, 2004. Primers YKO-up-F/YKO-up-R-T and YKO-down-F-T/YKO-down-R were respectively used to amplify the 520 bp up- and 573 bp down-stream homologous regions of the *rny* gene from Hp G27 WT gDNA. In parallel, the *aphA3* resistance cassette was amplified with oligos KmF and KmR on vector pNKO::Km^R. The rny_UP, Km^R and rny_DOWN PCR products were then mixed in a 1:3:1 ratio in a second PCR reaction and cycled for few times, to allow the extension and fusion of the three products. Finally, a third PCR reaction using YKO-up-F/YKO-down-R primers, allowed the amplification of the resulting 2424 bp product. 2 μg of the purified amplicon were then used to transform *H. pylori*. Transformants were selected on BA plates containing 25 μg/ml kanamycin and mutants were checked by sequencing the isolated gDNA.

5.6 Generation of the complemented Δ*rny* mutant strains

To complement the *rny* sequence or any of its mutated variants in a Hp G27 *rny* knock-out (Δ*rny*) background, we selected the *vacA* gene locus. Oligonucleotides 716-F_XbaI and 717-R_KpnI were used to amplify a 2.5 kb fragment encompassing the whole *rny*-HP0761 ORF with its promoter P_{761} and 113 bp of HP0762 CDS. The purified PCR product was then XbaI/KpnI cloned into pVAC::CAT, a pVAC::Km^R derivative carrying a BglII/BamHI *Campylobacter coli cat* chloramphenicol resistance cassette from pBS::*cat* (Vannini *et al.*, 2012). From the resulting pVAC::CAT-P_{761}-HP0761-*rny* a whole around PCR was performed with oligos Δ717wa_F and Δ717wa_R, the product was ligated and transformed into *E. coli* DH5α. The ensuing pVAC::CAT-P_{761}-*rny* construct carried an in-frame deletion of the *HP0761* gene, enabling us to complement the *rny* gene without introducing a secondary functional copy of *HP0761* gene.
Couples of primers YH374A-F/YH374A-R and ΔTMh_Fw/ΔTMh_Rev were then used to perform whole around PCRs on pVAC::CAT-P_{761}-*rny* template. The resulting products were blunt end ligated and cloned into *E. coli* DH5α to obtain the constructs pVAC::CAT-P_{761}-*rny*^{H374A} (harbouring a His-Ala mutation in position 374 of RNase Y aminoacidic sequence) and pVAC::CAT-P_{761}-*rny*$^{\Delta TMh}$ (harbouring a deletion for the first 26 amino acids of the RNase Y protein sequence).
Finally, primers Y_C-FLAG_Fw and Y_C-FLAG_Rev allowed us to generate pVAC::CAT-P_{761}-*rny*-FLAG and pVAC::CAT-P_{761}-*rny*$^{\Delta TMh}$-FLAG constructs, encoding for a RNase Y/ RNase Y$^{\Delta TMh}$-1x FLAG (Asp-Ile-Lys-Asp-Asp-Asp-Asp-Lys) fusion protein.
The constructs pVAC::CAT-P_{761}-*rny*, pVAC::CAT-P_{761}-*rny*^{H374A}, pVAC::CAT-P_{761}-*rny*-FLAG and pVAC::CAT-P_{761}-*rny*$^{\Delta TMh}$-FLAG were used to obtain respectively Hp G27 Δ*rny*::*rny*, Hp G27 Δ*rny*::*rny*^{H374A}, Hp G27 Δ*rny*::*rny*-FLAG and Hp G27::*rny*$^{\Delta TMh}$-FLAG mutant strains as stated above.

5.7 RNA preparation and RT-qPCR analysis

Unless otherwise stated, *H. pylori* was grown in liquid culture to exponential growth phase (OD_{600}=0.6-0.8). 10 ml of liquid cultures were harvested, mixed with 1.25 ml of ice-cold stop solution (95% ethanol + 5% water-saturated phenol pH 4.5) and immediately spun down at 5,000 g for 10 min at 4°C. Following the manufacturer's procedure, dry pellets were resuspended in 1 ml of Tri-Reagent™ and incubated 5 min at room temperature. Organic and aqueous phases were separated with the addition of 200 µl of chloroform and samples were centrifuged at 12000g for 10 min at 4°C. The upper aqueous phase was transferred to a fresh 2 ml tube and RNA was precipitated with the addition of 500 µl of isopropanol. Pellets were washed with 1 ml of 75% EtOH, resuspended in RNase-free mqH_2O and stored at -80°C in precipitation mix (1/10 volume of 3M NaOAc pH 5.2 and 2 volumes of cold 100% EtOH). Prior to use, an aliquot of each RNA sample was collected by centrifugation, quantified, and loaded on a 1% agarose gel to assess RNA purity and integrity.
Prior reverse transcription, 2µg of RNAs were treated with RapidOut DNA Removal kit (Thermo Fisher Scientific) following manufacturer's instructions, to eliminate residual genomic DNA. 500 ng of RNA were mixed with 100 pmol of Random Hexamers (Invitrogen) in a 12.5 µl reaction, denatured at 65°C for 5 min and rapidly chilled on ice. Then 200 U of RevertAid Reverse Transcriptase, 2 µl of dNTPs mix (10 mM each) and 4 µl of reaction buffer 5x were added in a final 20 µl reaction volume. Reactions were then incubated 10 min at 25°C and 60 min at 42°C. Reverse transcription reaction was terminated by heat inactivating the enzyme for 10 min at 70°C.
RT-qPCRs were carried out using PowerUp™ SYBR™ Green Master Mix (Applied Biosystems) with 50 pg of RNA per reaction. Relative gene expression was calculated using the $\Delta\Delta C_t$ method (Livak & Schmittgen, 2001) using the primers described in Table 3 and normalized on 16S rRNA otherwise differently specified.

5.8 Northern blot analysis

Table 3 provides a complete list of oligonucleotides used in hybridization experiments. 5 pmol of each primer was 5'-end labelled using 6 pmol of [γ-^{32}P]-ATP (Perkin-Elmer) with T4 polynucleotide kinase (New England Biolabs) at 37°C for 30 min. Unincorporated radiolabeled nucleotide was removed with a Bio-Spin Chromatography column (Bio-Rad) packed with Sephadex™ G-50 (Pharmacia Fine Chemicals). For Northern blot analysis of sRNAs, 10 µg of RNA was ethanol precipitated and resuspended in 10 µl of 2x RPA buffer (98% formamide + 0.025% Xylene cyan + 0.025% Bromophenol blue), denatured at 65°C for 10 min and rapidly chilled on ice. Samples were separated under denaturing conditions in 8M Urea, 6% Acrylamide/Bis 19:1 (Ambion) in 1x TBE buffer gel and transferred to a Hybond-N+ nylon membrane (Amersham) in 1x TBE buffer at 50V for 1 hour at 4°C. RNA samples were then crosslinked to the filter by UV-ray treatment (5 J, λ=356 nm). Membranes were prehybridized in 5 ml of ULTRAhyb™ Ultrasensitive Hybridization Buffer (Invitrogen) for 30 min and then hybridized in the same buffer with 1 pmol of radioactively labelled oligonucleotide at 42°C O/N. Finally, hybridized membranes were washed once with wash buffer I (5x SSC [1x SSC: 0.15 M NaCl, 0.015 M sodium citrate; pH 7.0], 0.1% SDS), once with wash buffer II (1x SSC, 0.1% SDS) and once with wash buffer III (0.1x SSC, 0.1% SDS). Each wash was performed for 15 min. Radioactive signal was acquired with a Storm phosphor-imager (Amersham-GE) and quantified using the Image Quant Software (Molecular Dynamics).

5.9 Primer extension analysis

Primer extension analyses were performed as previously described (Delany *et al.,* 2002). Briefly, 15-20 µg of RNA were ethanol precipitated and resuspended in 10 µl of primer extension reaction mix (0.1 pmol of radiolabeled primer, 400 nm dNTPs, in 1x Revert Aid buffer). After 2 min of denaturation at 95°C, 200U of Revert Aid Reverse Transcriptase (Invitrogen) were added and the reactions were incubated at 42°C for 1 h. After cDNA synthesis, reactions were incubated at room temperature with 1 µl of RNase A (10µg/µl), phenol-chloroform-isoamyl alcohol (25:24:1) extracted, ethanol precipitated and resuspended in 7 µl of formamide loading buffer (95% formamide, 0.1% bromophenol blue, 10 mM EDTA pH 8.0). Samples were denatured at 100 °C for 5 min, immediately chilled on ice, loaded on a 8M Urea, 6% Acrylamide/Bis (19:1) in 1x TBE buffer gel and run for 1h 30 min at 42 W. Gels were then dried and autoradiographed.
To ensure correct mapping of the investigated RNA 5' ends, a Sanger sequencing reaction was performed by using one of the primers used in primer extension reactions and the corresponding cloned promoter region (Delany *et al.,* 2002).

5.10 8xHis-MBP-MS2 fusion protein purification

Plasmid pHMM (Batey and Kieft, 2007) harbours the DNA sequence that encode for the 59 kDa 8xHis-MBP-MS2 fusion protein. This polypeptide is composed of an N-terminal octahistidine-tag, a maltose-binding protein (MBP) domain, and a C-terminal MS2 coat protein. The MS2-MBP protein purification was performed as described Lalaouna *et al.,* 2016 with slight modifications. E. coli BL21 (DE3) containing pHMM plasmid were grown in 100 ml of LB supplemented with 25 µg/ml kanamycin to an OD_{600}=0.6-0.7. Polypeptide overexpression was induced with the addition of 0.5 mM Isopropil-β-D-1-tiogalattopiranoside (IPTG) at 37°C in agitation (180 rpm) for 3 h. Cells were then collected by centrifugation (3800 g for 15 min at 4°C) and resuspended in 1.8 ml of Lysis buffer (50 mM NaH_2PO_4 pH=8.0, 300 mM NaCl, 0.5% Tween 20, 10mM Imidazole in 10% glycerol) supplemented with cOmplete Protease inhibitor cocktail (Roche) and 1 mg/ml of lysozyme. After 1 h of incubation at 4 °C in agitation, cells were lysed by sonication and centrifuged at 20,000g for 30 min at 4°C. The supernatant was transferred in a fresh 2 ml tube where 250 µl of Ni-NTA agarose resin (Thermo Fisher) previously equilibrated with lysis buffer were used to purify 8xHis-MBP-MS2 protein. After 1 h of incubation in agitation at 4°C the matrix was washed 3 times with 1 ml of lysis buffer and eluted with 1 ml of elution buffer. After an O/N dialysis against 1 L of dialysis buffer (25 mM HEPES pH = 6.0, 25 mM NaCl), the fusion protein was further purified using 250 µl of Amylose resin (New England Biolabs) previously equilibrated with 2 ml of column buffer (20 mM Tris-HCl pH=7.4, 200 mM NaCl 0.5 mM EDTA). Samples were eluted with 1 ml of column buffer + 10 mM maltose, dialysed twice against 500 ml of buffer A (20mM Tris-HCl pH=8.0, 150mM KCl, 1mM $MgCl_2$) and stored in aliquots at -80°C.
Protein purity was assessed by SDS-PAGE and its concentration was estimated by Bradford colorimetric assay (Bio-Rad).

5.11 MS2 based affinity chromatography

To perform the MS2 based affinity chromatography, *H. pylori* cells were grown in BB supplemented with 7.5% FCS and Dent's antibiotic mix as specified above. 210 ml of cells were harvested in mid-exponential phase of growth (OD_{600} = 0.6-0.8). 10 ml of cells were collected before affinity chromatography and the extracted RNA was used as input sample. The

remaining 200 ml were centrifuged and resuspended in 2 ml of buffer A supplemented with 1 mM Dithiothreitol (DTT) and 1 mM Phenylmethylsulfonyl fluoride (PMSF) freshly prepared. Cells were then pelleted again, resuspended in 8 ml of buffer A and lysed using a French Press cell disruptor with the following parameters: 500 psi, two times. The lysate was then cleared by centrifugation at 20,000g for 30 min at 4°C) and subjected to affinity chromatography.
150 pmol of 8xHis-MBP-MS2 protein were immobilized for 1 h at 4°C in agitation on 100 µl of Amylose resin (New England Biolabs) previously equilibrated in 1.5 ml of buffer A. After 2 wash steps with 1 ml of buffer A, the Amylose resin conjugated with 8xHis-MBP-MS2 was loaded in a Bio-Spin Chromatography column (Bio-Rad). The column was then washed twice with 2 ml of buffer A. The cleared lysate was loaded on the column before being washed two times with buffer A. RNA was eluted with 1 ml of buffer A + 15 mM maltose, extracted with 1V of PCI and ethanol precipitated O/N supplemented with 1 µl of RNA-grade glycogen 20 µg/ml (Invitrogen). RNA samples were then treated with RapidOut DNA Removal kit (Thermo Fisher Scientific) and reverse transcribed with RevertAid Reverse Transcriptase as stated above. RT-qPCR were performed to check the relative enrichments by using the $\Delta\Delta C_t$ method. Data were normalized on input samples obtained from ΔcncR1::MS2-term and ΔcncR1::cncR1 strains.

5.12 Probe preparation and DNase I footprinting

The promoter region of the HP0761-HP0760 operon was amplified with oligos AD_HP0761_RTF and AD_HP0761_R, and cloned in pGEM vector, obtaining pGEM-P*hp0761*. 1 pmol of pGEM-P*hp0761* vector was linearized with NdeI, dephosphorylated with calf intestinal phosphatase and labeled at the 5′ ends with 2 pmol of [γ-^{32P}] ATP (6,000 Ci/mmol; PerkinElmer) by using T4 polynucleotide kinase. The labeled DNA probe was further digested with NcoI and the products were separated by native polyacrylamide 6% gel electrophoresis and eluted in 1.5 ml of elution buffer (10 mM TrisHCl, pH 8.0, 1 mM EDTA, 300 mM sodium acetate, pH 5.2, 0.2% SDS) at 37°C overnight. The eluted probes were then extracted once with an equal volume of phenol–chloroform (1:1), ethanol precipitated and resuspended in 50 ml of milliQ water. The binding reactions between approximately 20 fmol of labeled probe and increasing concentrations of Fur were carried out at room temperature for 15 min in a final volume of 50 µl in the footprinting buffer (10 mM Tris-HCl, pH 7.85, 50 mM NaCl, 10 mM KCl, 0.02% Igepal CA-630, 10% glycerol, 5 mM dithiothreitol) containing an excess of $(NH_4)_2Fe(SO_4)_2$ (150 µM) or 2,2-dipyridyl (150 µM) and with 300 ng of salmon sperm DNA (Invitrogen) as a nonspecific competitor. Afterwards, DNase I (0.08 U), diluted in footprinting buffer 1X containing 10 mM $CaCl_2$ and 5 mM $MgCl_2$ was added to the reaction mixture and digestion was allowed to occur for 85 s. The reaction was stopped by adding 140 µl of stop buffer (192 mM NaOAc pH 5.2, 32 mM EDTA pH 8.0, 0.14 % SDS, 64 µg/ml sonicated salmon sperm DNA), extracted once with an equal volume of phenol–chloroform (1:1), ethanol precipitated and resuspended in 5 µl of formamide loading buffer. Samples were denatured at 100°C for 3 min, separated on 8 M urea-6% acrylamide sequencing gels in TBE buffer and autoradiographed. A modified G+A sequencing ladder protocol (Liu and Hong, 1998) was employed to map the binding sites.

5.13 Cellular fractionation of H. pylori

The cellular fractionation protocol was adapted from Tejada-Arranz *et al.*, 2020. Briefly, 50 ml of *H. pylori* Δ*rny*::*rny*-FLAG and Δ*rny*::*rny*$^{\Delta TMh}$-FLAG liquid cultures were grown up to mid-exponential phase (OD_{600}= 0.6-0.7) and harvested by centrifugation at 5,000 g for 10 min at

4°C. Cells were washed with PBS, collected again by centrifugation and resuspended to an OD_{600} = 5 in a lysis buffer containing 10 mM Tris-HCl (pH 7.4) and Complete protease inhibitor cocktail (Roche) (buffer I).Then, bacterial cells were disrupted by sonication, cell debris were removed by centrifugation at 20,000g for 30 min at 4°C and the supernatants were collected as total extracts (TE). 5 ml of supernatants were transferred to 5 ml ultracentrifuge tubes (Beckman Coulter Life Sciences) and centrifuged at 100,000 g for 45 min at 4°C in a Optima L-90K ultracentrifuge using a 50.3Ti rotor (Beckman Coulter Life Sciences). The supernatants contained the cytosolic soluble (Cs) fraction, while the pellets corresponded to the total membranes. Pellets were washed twice with 1 ml of buffer I, resuspended in 5 ml of buffer I + 0.1% N-lauroylsarcosine (Sigma Aldrich) and ultracentrifuged again in the same conditions. The supernatants containing the inner membrane (IM) fraction were collected and the pellets containing the outer membrane (OM) fraction were resuspended in 5 ml of buffer I + 1% N-lauroylsarcosine. Western blots with specific antibodies for Cs and OM fractions (i.e., α-HP1043 and α-BabA, respectively) were performed as a control of the correct separations of the different fractions as specified below.

5.14 Western blot analysis

16 µl of each *H. pylori* fraction (prepared as described above) with the addition of 4 µl of 5x Laemmli buffer were denatured for 10 minutes at 100 °C, rapidly chilled on ice, loaded and separated under denaturing conditions on a 10% Acrylamide/Bis 29:1 (Ambion) in 1x Tris-glycine SDS buffer (25mM tris, 192 mM, 0.1% SDS). Proteins were then transferred to a Amersham™ Hybond™ PVDF membrane (GE Helathcare Life scince) previously activated for 30s in methanol, washed for 2 min in mqH_2O and 10 min in transfer buffer (50 mM Tris, 200mM glycine, 20%methanol) with the Trans-Blot® Turbo™ (BioRad) semi-dry system. The *H. pylori* HP1043, BabA proteins were detected with rabbit polyclonal antibodies α-HP1043 and α-BabA at 1:5000 and 1:10000 dilutions, respectively. RNase Y-FLAG protein was detected with mouse polyclonal α-FLAG antibody at 1:1000 dilution. Goat α-rabbit IgG-HRP or goat α-mouse IgG-HRP were used as secondary antibodies at 1:10000 dilution. LightWave™ Max ECL (GVS) was used for the detection and the signal was acquired with a ChemiDoc™ MP Imaging System (BioRad).

5.15 RNA-sequencing and Data Analysis

H. pylori G27 liquid cultures of wild type and Δ*rny* strains were grown until mid-exponential phase (OD_{600} = 0.6). Then, 10 ml of liquid cultures were harvested, mixed with 1.25 ml of ice-cold stop solution (95% ethanol + 5% water-saturated phenol pH 4.5) and immediately spun down at 5,000 g for 10 min at 4°C. Total RNA was extracted with TRI-reagent™ (Invitrogen) following manufacturer's instructions. Ribosomal RNA depletion, quality check and strand specific cDNAs library preparation were all performed starting from 2 µg of total RNA through the Novogene company service. Each library was sequenced on an Illumina NovaSeq 6000 platform and 150 bp paired-end reads were produced. Bowtie 2 (v2.2.6) was used to align raw reads to H. pylori G27 genome. End-to-end mapping was performed, and non-deterministic option was specified to force a single assignment of multi-mapping reads to the best scoring region (if present) or a random attribution in the case of regions with identical scores. High quality reads were selected requiring both read of the pair to be mapped, for uniquely mapping reads MAPQ (mapping quality) greater than 20; while for multi-mapping reads alignment score was set equal or greater than − 25 rRNA depletion, strand specificity and gene coverage were evaluated using BEDTools (v2.20.1*) and SAMtools (v0.1.19) to verify the library preparation

and sequencing performances. FeatureCounts was adopted to produce raw counts requiring strand specificity of the read pair and -d 20 -D 1200 to include also reads with non-standard length of the pair occurring for example in tRNA and ncRNA transcripts. Read pairs overlapping multiple features were excluded. The R package DESeq2 (v1.4.5) was then used to normalize the counts and to individuate differentially expressed features showing BH (Benjamini-Hochberg) adjusted p-value lower than 0.01 and log2 Fold Change >|1|. COG functional enrichments were estimated using Hypergeometric Test and BH correction for multiple testing.

5.16 DNA manipulations

DNA amplification, restriction digestions and ligations were all performed with enzymes purchased from New England Biolabs, by following standard molecular procedures (Sambrook *et al.*, 1989). DNA fragments purification from agarose gels or from PCR reactions were carried out with a NucleoSpin™ Gel an PCR Clean-up kit (Macherey-Nagel). Plasmid DNA preparations were realized with a NucleoSpin™ Plasmid (Macherey-Nagel).

5.17 Bioinformatic analyses

The InterPro (https://www.ebi.ac.uk/interpro/) predictor was used to obtain a comprehensive prediction of the functional domains of the RNase Y protein.
The DeepTMHMM (https://dtu.biolib.com/DeepTMHMM) and Phobius (https://phobius.sbc.su.se/) online resources were used to predict the transmembrane domain in the RNase Y aminoacidic sequence.
The RNAfold (http://rna.tbi.univie.ac.at/cgi-bin/RNAWebSuite/RNAfold.cgi) online program was used to predict the secondary structure of RNA sequences.
The Alphafold (https://alphafold.ebi.ac.uk/) database was used to obtain the structure prediction for the RNase Y protein.
The Paircoil2 (https://cb.csail.mit.edu/cb/paircoil2/) and Marcoil (http://bcf.isb-sib.ch/webmarcoil/webmarcoilINFOC1.html) online programs were used to identify coiled coil regions on the RNase Y aminoacidic sequence.

6. References

Alm, R. A., Ling, L. S. L., Moir, D. T., King, B. L., Brown, E. D., Doig, P. C., Smith, D. R., Noonan, B., Guild, B. C., DeJonge, B. L., Carmel, G., Tummino, P. J., Caruso, A., Uria-Nickelsen, M., Mills, D. M., Ives, C., Gibson, R., Merberg, D., Mills, S. D., … Trust, T. J. (1999). Genomic-sequence comparison of two unrelated isolates of the human gastric pathogen Helicobacter pylori. *Nature*, *397*(6715), 176–180. https://doi.org/10.1038/16495

Aravind, L., & Koonin, E. v. (1998). The HD domain defines a new superfamily of metal-dependent phosphohydrolases. *Trends in Biochemical Sciences*, *23*(12), 469–472. https://doi.org/10.1016/S0968-0004(98)01293-6

Baltrus, D. A., Amieva, M. R., Covacci, A., Lowe, T. M., Merrell, D. S., Ottemann, K. M., Stein, M., Salama, N. R., & Guillemin, K. (**2009**). The complete genome sequence of Helicobacter pylori strain G27. *Journal of Bacteriology*, *91*(1), 447–448. https://doi.org/10.1128/JB.01416-08

Baltrus, D. A., Amieva, M. R., Covacci, A., Lowe, T. M., Merrell, D. S., Ottemann, K. M., Stein, M., Salama, N. R., & Guillemin, K. (**2009**). The complete genome sequence of Helicobacter pylori strain G27. *Journal of Bacteriology*, *91*(1), 447–448. https://doi.org/10.1128/JB.01416-08

Batey, R. T., & Kieft, J. S. (**2007**). Improved native affinity purification of RNA. *RNA (New York, N.Y.)*, *13*(8), 1384–1389. https://doi.org/10.1261/RNA.528007

Behrens, W., Bönig, T., Suerbaum, S., & Josenhans, C. (2012). Genome sequence of Helicobacter pylori hpEurope strain N6. *Journal of Bacteriology*, *194*(14), 3725–3726. https://doi.org/10.1128/JB.00386-12

Bereswill, S., Lichte, F., Vey, T., Fassbinder, F., & Kist, M. (1998). Cloning and characterization of the fur gene from Helicobacter pylori . *FEMS Microbiology Letters*, *159*(2), 193–200. https://doi.org/10.1111/J.1574-6968.1998.TB12860.X

Bereswill, S., Greiner, S., van Vliet, A. H. M., Waidner, B., Fassbinder, F., Schiltz, E., Kusters, J. G., & Kist, M. (2000). Regulation of ferritin-mediated cytoplasmic iron storage by the ferric uptake regulator homolog (Fur) of Helicobacter pylori. *Journal of Bacteriology*, *182*(21), 5948–5953. https://doi.org/10.1128/JB.182.21.5948-5953.2000

Brahmachary, P., Dashti, M. G., Olson, J. W., & Hoover, T. R. (2004). Helicobacter pylori FlgR is an enhancer-independent activator of sigma54-RNA polymerase holoenzyme. *Journal of Bacteriology*, *186*(14), 4535–4542. https://doi.org/10.1128/JB.186.14.4535-4542.2004

Broglia, L., Lécrivain, A. L., Renault, T. T., Hahnke, K., Ahmed-Begrich, R., le Rhun, A., & Charpentier, E. (2020). An RNA-seq based comparative approach reveals the transcriptome-wide interplay between 3′-to-5′ exoRNases and RNase Y. *Nature Communications*, *11*(1). https://doi.org/10.1038/s41467-020-15387-6

Bugrysheva, J. v., & Scott, J. R. (2010). The ribonucleases J1 and J2 are essential for growth and have independent roles in mRNA decay in Streptococcus pyogenes. *Molecular Microbiology*, *75*(3), 731–743. https://doi.org/10.1111/J.1365-2958.2009.07012.X

Carrier, M. C., Lalaouna, D., & Massé, E. (2016). A game of tag: MAPS catches up on RNA interactomes. *RNA Biology*, *13*(5), 473–476. https://doi.org/10.1080/15476286.2016.1156830

Carrier, M. C., Lalaouna, D., & Massé, E. (2018). Broadening the Definition of Bacterial Small RNAs: Characteristics and Mechanisms of Action. *Annual Review of Microbiology*, *72*, 141–161. https://doi.org/10.1146/ANNUREV-MICRO-090817-062607

Castillo, A. R., Arevalo, S. S., Woodruff, A. J., & Ottemann, K. M. (2008). Experimental analysis of Helicobacter pylori transcriptional terminators suggests this microbe uses both intrinsic and factor-dependent termination. *Molecular Microbiology*, *67*(1), 155–170. https://doi.org/10.1111/J.1365-2958.2007.06033.X

Chao, Y., & Vogel, J. (2016). A 3' UTR-Derived Small RNA Provides the Regulatory Noncoding Arm of the Inner Membrane Stress Response. *Molecular Cell*, *61*(3), 352–363. https://doi.org/10.1016/J.MOLCEL.2015.12.023

Chao, Y., Li, L., Girodat, D., Förstner, K. U., Said, N., Corcoran, C., Śmiga, M., Papenfort, K., Reinhardt, R., Wieden, H. J., Luisi, B. F., & Vogel, J. (2017). In Vivo Cleavage Map Illuminates the Central Role of RNase E in Coding and Non-coding RNA Pathways. *Molecular Cell*, *65*(1), 39–51. https://doi.org/10.1016/J.MOLCEL.2016.11.002

Chen, Z., Itzek, A., Malke, H., Ferretti, J. J., & Kreth, J. (2013). Multiple roles of RNase Y in Streptococcus pyogenes mRNA processing and degradation. *Journal of Bacteriology*, *195*(11), 2585–2594. https://doi.org/10.1128/JB.00097-13

Chevalier, C., Thiberge, J. M., Ferrero, R. L., & Labigne, A. (1999). Essential role of Helicobacter pylori γ-glutamyltranspeptidase for the colonization of the gastric mucosa of mice. *Molecular Microbiology*, *31*(5), 1359–1372. https://doi.org/10.1046/j.1365-2958.1999.01271.x

Contreras, M., Thiberge, J. M., Mandrand-Berthelot, M. A., & Labigne, A. (2003). Characterization of the roles of NikR, a nickel-responsive pleiotropic autoregulator of Helicobacter pylori. *Molecular Microbiology*, *49*(4), 947–963. https://doi.org/10.1046/J.1365-2958.2003.03621.X

Danielli, A., Roncarati, D., Delany, I., Chiarini, V., Rappuoli, R., & Scarlato, V. (2006). In vivo dissection of the Helicobacter pylori Fur regulatory circuit by genome-wide location analysis. *Journal of Bacteriology*, *188*(13), 4654–4662. https://doi.org/10.1128/JB.00120-06

de la Cruz, M. A., Ares, M. A., Bargen, K. von, Panunzi, L. G., Martínez-Cruz, J., Valdez-Salazar, H. A., Jiménez-Galicia, C., & Torres, J. (2017). Gene Expression Profiling of Transcription Factors of Helicobacter pylori under Different Environmental Conditions. *Frontiers in Microbiology*, *8*(APR). https://doi.org/10.3389/FMICB.2017.00615

Delany, I., Pacheco, A. B. F., Spohn, G., Rappuoli, R., & Scarlato, V. (2001a). Iron-dependent transcription of the frpB gene of Helicobacter pylori is controlled by the Fur repressor

protein. *Journal of Bacteriology*, *183*(16), 4932–4937. https://doi.org/10.1128/JB.183.16.4932-4937.2001

Delany, I., Spohn, G., Rappuoli, R., & Scarlato, V. (2001b). The Fur repressor controls transcription of iron-activated and -repressed genes in Helicobacter pylori. *Molecular Microbiology*, *42*(5), 1297–1309. https://doi.org/10.1046/J.1365-2958.2001.02696.X

Delany, I., Spohn, G., Rappuoli, R., & Scarlato, V. (2002a). Growth phase-dependent regulation of target gene promoters for binding of the essential orphan response regulator HP1043 of Helicobacter pylori. *Journal of Bacteriology*, *184*(17), 4800–4810. https://doi.org/10.1128/JB.184.17.4800-4810.2002

Delany, I., Spohn, G., Pacheco, A. B. F., Ieva, R., Alaimo, C., Rappuoli, R., & Scarlato, V. (2002b). Autoregulation of Helicobacter pylori Fur revealed by functional analysis of the iron-binding site. *Molecular Microbiology*, *46*(4), 1107–1122. https://doi.org/10.1046/J.1365-2958.2002.03227.X

DeLoughery, A., Lalanne, J. B., Losick, R., & Li, G. W. (2018). Maturation of polycistronic mRNAs by the endoribonuclease RNase Y and its associated Y-complex in Bacillus subtilis. *Proceedings of the National Academy of Sciences of the United States of America*, *115*(24), E5585–E5594. https://doi.org/10.1073/PNAS.1803283115/-/DCSUPPLEMENTAL

Deutscher, M. P. (2015). How bacterial cells keep ribonucleases under control. *FEMS Microbiology Reviews*, *39*(3), 350–361. https://doi.org/10.1093/FEMSRE/FUV012

Donczew, R., Makowski, L., Jaworski, P., Bezulska, M., Nowaczyk, M., Zakrzewska-Czerwińska, J., & Zawilak-Pawlik, A. (2015). The atypical response regulator HP1021 controls formation of the Helicobacter pylori replication initiation complex. *Molecular Microbiology*, *95*(2), 297–312. https://doi.org/10.1111/MMI.12866

Du, M. Q., & Isaccson, P. G. (2002). Gastric MALT lymphoma: From aetiology to treatment. *Lancet Oncology*, *3*(2), 97–104. https://doi.org/10.1016/S1470-2045(02)00651-4

Durand, S., & Condon, C. (2018). RNases and Helicases in Gram-Positive Bacteria. *Microbiology Spectrum*, *6*(2). https://doi.org/10.1128/microbiolspec.rwr-0003-2017

Durand, S., Gilet, L., Bessières, P., Nicolas, P., & Condon, C. (2012). Three essential ribonucleases-RNase Y, J1, and III-control the abundance of a majority of Bacillus subtilis mRNAs. *PLoS Genetics*, *8*(3). https://doi.org/10.1371/JOURNAL.PGEN.1002520

Durand, S., Tomasini, A., Braun, F., Condon, C., & Romby, P. (2015). sRNA and mRNA turnover in Gram-positive bacteria. *FEMS Microbiology Reviews*, *39*(3), 316–330. https://doi.org/10.1093/FEMSRE/FUV007

Eisenbart, S. K., Alzheimer, M., Pernitzsch, S. R., Dietrich, S., Stahl, S., & Sharma, C. M. (2020). A Repeat-Associated Small RNA Controls the Major Virulence Factors of Helicobacter pylori. *Molecular Cell*, *80*(2), 210-226.e7. https://doi.org/10.1016/J.MOLCEL.2020.09.009

Foynes, S., Dorrell, N., Ward, S. J., Stabler, R. A., McColm, A. A., Rycroft, A. N., & Wren, B. W. (2000). Helicobacter pylori possesses two CheY response regulators and a histidine kinase sensor, CheA, which are essential for chemotaxis and colonization of the gastric mucosa. *Infection and Immunity*, *68*(4), 2016–2023. https://doi.org/10.1128/IAI.68.4.2016-2023.2000

Fröhlich, K. S., Haneke, K., Papenfort, K., & Vogel, J. (2016). The target spectrum of SdsR small RNA in Salmonella. *Nucleic Acids Research*, *44*(21), 10406–10422. https://doi.org/10.1093/NAR/GKW632

Georg, J., & Hess, W. R. (2011). cis -Antisense RNA, Another Level of Gene Regulation in Bacteria . *Microbiology and Molecular Biology Reviews*, *75*(2), 286–300. https://doi.org/10.1128/mmbr.00032-10

Gilet, L., Dichiara, J. M., Figaro, S., Bechhofer, D. H., & Condon, C. (2015). Small stable RNA maturation and turnover in Bacillus subtilis. *Molecular Microbiology*, *95*(2), 270–282. https://doi.org/10.1111/MMI.12863

Gorski, S. A., Vogel, J., & Doudna, J. A. (2017). RNA-based recognition and targeting: sowing the seeds of specificity. *Nature Reviews. Molecular Cell Biology*, *18*(4), 215–228. https://doi.org/10.1038/NRM.2016.174

Hamouche, L., Billaudeau, C., Rocca, A., Chastanet, A., Ngo, S., Laalami, S., & Putzer, H. (2020). Dynamic membrane localization of RNase Y in bacillus subtilis. *MBio*, *11*(1). https://doi.org/10.1128/mBio.03337-19

Hanahan, D. (1983). Studies on transformation of Escherichia coli with plasmids. *Journal of Molecular Biology*, *166*(4), 557–580. https://doi.org/10.1016/S0022-2836(83)80284-8

Hooi, J. K. Y., Lai, W. Y., Ng, W. K., Suen, M. M. Y., Underwood, F. E., Tanyingoh, D., Malfertheiner, P., Graham, D. Y., Wong, V. W. S., Wu, J. C. Y., Chan, F. K. L., Sung, J. J. Y., Kaplan, G. G., & Ng, S. C. (2017). Global Prevalence of Helicobacter pylori Infection: Systematic Review and Meta-Analysis. *Gastroenterology*, *153*(2), 420–429. https://doi.org/10.1053/j.gastro.2017.04.022

Iost, I., Chabas, S., & Darfeuille, F. (2019). Maturation of atypical ribosomal RNA precursors in Helicobacter pylori. *Nucleic Acids Research*, *47*(11), 5906–5921. https://doi.org/10.1093/NAR/GKZ258

Jain, C., & Belasco, J. G. (1995). RNase E autoregulates its synthesis by controlling the degradation rate of its own mRNA in Escherichia coli: Unusual sensitivity of the rne transcript to RNase E activity. *Genes and Development*, *9*(1), 84–96. https://doi.org/10.1101/gad.9.1.84

Jumper, J., Evans, R., Pritzel, A., Green, T., Figurnov, M., Ronneberger, O., Tunyasuvunakool, K., Bates, R., Žídek, A., Potapenko, A., Bridgland, A., Meyer, C., Kohl, S. A. A., Ballard, A. J., Cowie, A., Romera-Paredes, B., Nikolov, S., Jain, R., Adler, J., … Hassabis, D. (2021). Highly accurate protein structure prediction with AlphaFold. *Nature*, *596*(7873), 583–589. https://doi.org/10.1038/s41586-021-03819-2

Kayali, S., Manfredi, M., Gaiani, F., Bianchi, L., Bizzarri, B., Leandro, G., di Mario, F., & De'angelis, G. L. (2018). Helicobacter pylori, transmission routes and recurrence of

infection: state of the art. *Acta Bio-Medica : Atenei Parmensis*, *89*(8-S), 72–76. https://doi.org/10.23750/ABM.V89I8-S.7947

Khemici, V., Poljak, L., Luisi, B. F., & Carpousis, A. J. (2008). The RNase E of Escherichia coli is a membrane-binding protein. *Molecular Microbiology*, *70*(4), 799–813. https://doi.org/10.1111/j.1365-2958.2008.06454.x

Khemici, V., Prados, J., Linder, P., & Redder, P. (2015). Decay-Initiating Endoribonucleolytic Cleavage by RNase Y Is Kept under Tight Control via Sequence Preference and Sub-cellular Localisation. *PLoS Genetics*, *11*(10). https://doi.org/10.1371/JOURNAL.PGEN.1005577

Kinoshita-Daitoku, R., Kiga, K., Miyakoshi, M., Otsubo, R., Ogura, Y., Sanada, T., Bo, Z., Phuoc, T. V., Okano, T., Iida, T., Yokomori, R., Kuroda, E., Hirukawa, S., Tanaka, M., Sood, A., Subsomwong, P., Ashida, H., Binh, T. T., Nguyen, L. T., … Mimuro, H. (2021). A bacterial small RNA regulates the adaptation of Helicobacter pylori to the host environment. *Nature Communications*, *12*(1). https://doi.org/10.1038/S41467-021-22317-7

Laalami, S., Zig, L., & Putzer, H. (2014). Initiation of mRNA decay in bacteria. *Cellular and Molecular Life Sciences*, *71*(10), 1799–1828. https://doi.org/10.1007/s00018-013-1472-4

Lalaouna, D., Carrier, M. C., Semsey, S., Brouard, J. S., Wang, J., Wade, J. T., & Massé, E. (2015). A 3' external transcribed spacer in a tRNA transcript acts as a sponge for small RNAs to prevent transcriptional noise. *Molecular Cell*, *58*(3), 393–405. https://doi.org/10.1016/J.MOLCEL.2015.03.013

Lalaouna, D., Morissette, A., Carrier, M. C., & Massé, E. (2015). DsrA regulatory RNA represses both hns and rbsD mRNAs through distinct mechanisms in Escherichia coli. *Molecular Microbiology*, *98*(2), 357–369. https://doi.org/10.1111/MMI.13129

Lalaouna, D., Prévost, K., Eyraud, A., & Massé, E. (2017). Identification of unknown RNA partners using MAPS. *Methods (San Diego, Calif.)*, *117*, 28–34. https://doi.org/10.1016/J.YMETH.2016.11.011

Lehnik-Habrink, M., Newman, J., Rothe, F. M., Solovyova, A. S., Rodrigues, C., Herzberg, C., Commichau, F. M., Lewis, R. J., & Stülke, J. (2011). RNase Y in Bacillus subtilis: a Natively disordered protein that is the functional equivalent of RNase E from Escherichia coli. *Journal of Bacteriology*, *193*(19), 5431–5441. https://doi.org/10.1128/JB.05500-11

Lehnik-Habrink, M., Pförtner, H., Rempeters, L., Pietack, N., Herzberg, C., & Stülke, J. (2010). The RNA degradosome in Bacillus subtilis: identification of CshA as the major RNA helicase in the multiprotein complex. *Molecular Microbiology*, *77*(4), 958–971. https://doi.org/10.1111/J.1365-2958.2010.07264.X

Lim, B., Sim, M., Lee, H., Hyun, S., Lee, Y., Hahn, Y., Shin, E., & Lee, K. (2015). Regulation of Escherichia coli RNase III activity. *Journal of Microbiology*, *53*(8), 487–494. https://doi.org/10.1007/s12275-015-5323-x

Livak, K. J., & Schmittgen, T. D. (2001). Analysis of relative gene expression data using real-time quantitative PCR and the 2(-Delta Delta C(T)) Method. *Methods (San Diego, Calif.)*, *25*(4), 402–408. https://doi.org/10.1006/METH.2001.1262

Loh, J. T., Shum, M. v., Jossart, S. D. R., Campbell, A. M., Sawhney, N., Hayes McDonald, W., Scholz, M. B., McClain, M. S., Forsyth, M. H., & Cover, T. L. (2021). Delineation of the pH-Responsive Regulon Controlled by the Helicobacter pylori ArsRS Two-Component System. *Infection and Immunity*, *89*(4). https://doi.org/10.1128/IAI.00597-20

Mackie, G. A. (2013). RNase E: at the interface of bacterial RNA processing and decay. *Nature Reviews. Microbiology*, *11*(1), 45–57. https://doi.org/10.1038/NRMICRO2930

Malfertheiner, P., Megraud, F., O'Morain, C., Bazzoli, F., El-Omar, E., Graham, D., Hunt, R., Rokkas, T., Vakil, N., Kuipers, E. J., Andersen, L., Atherton, J., Asaka, M., Bazzoli, F., Bytzer, P., Chan, F., Coelho, L. G. V., de Wit, N., Delchier, J. C., … Xiao, S. (2007). Current concepts in the management of helicobacter pylori infection: The maastricht III consensus report. *Gut*, *56*(6), 772–781. https://doi.org/10.1136/gut.2006.101634

Malfertheiner, P., Megraud, F., O'Morain, C., Gisbert, J. P., Kuipers, E. J., Axon, A., Bazzoli, F., Gasbarrini, A., Atherton, J., Graham, D. Y., Hunt, R., Moayyedi, P., Rokkas, T., Rugge, M., Selgrad, M., Suerbaum, S., Sugano, K., El-Omar, E., Agreus, L., … You, W. (2017). Management of Helicobacter pylori infection-the Maastricht V/Florence Consensus Report. *Gut*, *66*(1), 6–30. https://doi.org/10.1136/GUTJNL-2016-312288

Mao, F., Dam, P., Chou, J., Olman, V., & Xu, Y. (2009). DOOR: a database for prokaryotic operons. *Nucleic Acids Research*, *37*(Database issue). https://doi.org/10.1093/NAR/GKN757

Marincola, G., & Wolz, C. (2017). Downstream element determines RNase Y cleavage of the saePQRS operon in Staphylococcus aureus. *Nucleic Acids Research*, *45*(10), 5980–5994. https://doi.org/10.1093/NAR/GKX296

Marshall, B. J., & Warren, J. R. (1984). Unidentified curved bacilli in the stomach of patients with gastritis and peptic ulceration. *Lancet (London, England)*, *1*(8390), 1311–1315. https://doi.org/10.1016/S0140-6736(84)91816-6

Matsunaga, J., Simons, E. L., & Simons, R. W. (1997). Escherichia coli RNase III (rnc) autoregulation occurs independently of rnc gene translation. *Molecular Microbiology*, *26*(5), 1125–1135. https://doi.org/10.1046/J.1365-2958.1997.6652007.X

Moffitt, J. R., Pandey, S., Boettiger, A. N., Wang, S., & Zhuang, X. (2016). Spatial organization shapes the turnover of a bacterial transcriptome. *ELife*, *5*(MAY2016). https://doi.org/10.7554/ELIFE.13065

Mohanty, B. K., & Kushner, S. R. (2016). Regulation of mRNA Decay in Bacteria. *Annual Review of Microbiology*, *70*, 25–44. https://doi.org/10.1146/ANNUREV-MICRO-091014-104515

Mortaji, L. el, Tejada-Arranz, A., Rifflet, A., Boneca, I. G., Pehau-Arnaudet, G., Radicella, J. P., Marsin, S., & de Reuse, H. (2020). A peptide of a type I toxin-antitoxin system induces Helicobacter pylori morphological transformation from spiral shape to coccoids. *Proceedings of the National Academy of Sciences of the United States of America*, *117*(49), 31398–31409. https://doi.org/10.1073/PNAS.2016195117/-/DCSUPPLEMENTAL

Nicastro, G., Taylor, I. A., & Ramos, A. (2015). KH-RNA interactions: back in the groove. *Current Opinion in Structural Biology*, *30*, 63–70. https://doi.org/10.1016/J.SBI.2015.01.002

Niehus, E., Gressmann, H., Ye, F., Schlapbach, R., Dehio, M., Dehio, C., Stack, A., Meyer, T. F., Suerbaum, S., & Josenhans, C. (2004). Genome-wide analysis of transcriptional hierarchy and feedback regulation in the flagellar system of Helicobacter pylori. *Molecular Microbiology*, *52*(4), 947–961. https://doi.org/10.1111/J.1365-2958.2004.04006.X

Nomura, A., Stemmermann, G. N., Chyou, P. H., Perez-Perez, G. I., & Blaser, M. J. (1994). Helicobacter pylori infection and the risk for duodenal and gastric ulceration. *Annals of Internal Medicine*, *120*(12), 977–981. https://doi.org/10.7326/0003-4819-120-12-199406150-00001

Pelliciari, S., Pinatel, E., Vannini, A., Peano, C., Puccio, S., de Bellis, G., Danielli, A., Scarlato, V., & Roncarati, D. (2017). Insight into the essential role of the Helicobacter pylori HP1043 orphan response regulator: genome-wide identification and characterization of the DNA-binding sites. *Scientific Reports*, *7*. https://doi.org/10.1038/SREP41063

Pernitzsch, S. R., & Sharma, C. M. (2012). Transcriptome complexity and riboregulation in the human pathogen Helicobacter pylori. *Frontiers in Cellular and Infection Microbiology*, *2*, 14. https://doi.org/10.3389/FCIMB.2012.00014

Pernitzsch, S. R., Alzheimer, M., Bremer, B. U., Robbe-Saule, M., de Reuse, H., & Sharma, C. M. (2021). Small RNA mediated gradual control of lipopolysaccharide biosynthesis affects antibiotic resistance in Helicobacter pylori. *Nature Communications*, *12*(1). https://doi.org/10.1038/S41467-021-24689-2

Pernitzsch, S. R., Tirier, S. M., Beier, D., & Sharma, C. M. (2014). A variable homopolymeric G-repeat defines small RNA-mediated posttranscriptional regulation of a chemotaxis receptor in Helicobacter pylori. *Proceedings of the National Academy of Sciences of the United States of America*, *111*(4). https://doi.org/10.1073/PNAS.1315152111/-/DCSUPPLEMENTAL/SAPP.PDF

Pflock, M., Kennard, S., Delany, I., Scarlato, V., & Beier, D. (2005). Acid-induced activation of the urease promoters is mediated directly by the ArsRS two-component system of Helicobacter pylori. *Infection and Immunity*, *73*(10), 6437–6445. https://doi.org/10.1128/IAI.73.10.6437-6445.2005

Prévost, K., Salvail, H., Desnoyers, G., Jacques, J. F., Phaneuf, É., & Massé, E. (2007). The small RNA RyhB activates the translation of shiA mRNA encoding a permease of shikimate, a compound involved in siderophore synthesis. *Molecular Microbiology*, *64*(5), 1260–1273. https://doi.org/10.1111/J.1365-2958.2007.05733.X

Quendera, A. P., Seixas, A. F., dos Santos, R. F., Santos, I., Silva, J. P. N., Arraiano, C. M., & Andrade, J. M. (2020). RNA-Binding Proteins Driving the Regulatory Activity of Small Non-coding RNAs in Bacteria. *Frontiers in Molecular Biosciences*, *7*, 78. https://doi.org/10.3389/fmolb.2020.00078

Redko, Y., Aubert, S., Stachowicz, A., Lenormand, P., Namane, A., Darfeuille, F., Thibonnier, M., & de Reuse, H. (2013). A minimal bacterial RNase J-based degradosome is associated

with translating ribosomes. *Nucleic Acids Research*, *41*(1), 288–301. https://doi.org/10.1093/NAR/GKS945

Rieder, R., Reinhardt, R., Sharma, C. M., & Vogel, J. (2012). Experimental tools to identify RNA-protein interactions in Helicobacter pylori. *RNA Biology*, *9*(4), 520–531. https://doi.org/10.4161/RNA.20331

Robert-le Meur, M., & Portier, C. (1994). Polynucleotide phosphorylase of Escherichia coli induces the degradation of its RNase III processed messenger by preventing its translation. *Nucleic Acids Research*, *22*(3), 397–403. https://doi.org/10.1093/NAR/22.3.397

Roncarati, D., & Scarlato, V. (2018). The Interplay between Two Transcriptional Repressors and Chaperones Orchestrates Helicobacter pylori Heat-Shock Response. *International Journal of Molecular Sciences*, *19*(6). https://doi.org/10.3390/IJMS19061702

Roncarati, D., Pinatel, E., Fiore, E., Peano, C., Loibman, S., & Scarlato, V. (2019). Helicobacter pylori Stress-Response: Definition of the HrcA Regulon. *Microorganisms*, *7*(10). https://doi.org/10.3390/MICROORGANISMS7100436

Saliba, A. E., C Santos, S., & Vogel, J. (2017). New RNA-seq approaches for the study of bacterial pathogens. *Current Opinion in Microbiology*, *35*, 78–87. https://doi.org/10.1016/J.MIB.2017.01.001

Sambrook, J.E.F.F., and T. Maniatis (1989). Molecular cloning: a laboratory manual. In, C.S.H. Cold Spring Harbor Laboratory, NY, ed

Saramago, M., Bárria, C., dos Santos, R. F., Silva, I. J., Pobre, V., Domingues, S., Andrade, J. M., Viegas, S. C., & Arraiano, C. M. (2014). The role of RNases in the regulation of small RNAs. *Current Opinion in Microbiology*, *18*(1), 105–115. https://doi.org/10.1016/J.MIB.2014.02.009

Scarlato, V., Delany, I., Spohn, G., & Beier, D. (2001). Regulation of transcription in Helicobacter pylori: simple systems or complex circuits? *International Journal of Medical Microbiology : IJMM*, *291*(2), 107–117. https://doi.org/10.1078/1438-4221-00107

Schuck, A., Diwa, A., & Belasco, J. G. (2009). RNase E autoregulates its synthesis in Escherichia coli by binding directly to a stem-loop in the rne 5' untranslated region. *Molecular Microbiology*, *72*(2), 470–478. https://doi.org/10.1111/J.1365-2958.2009.06662.X

Shahbabian, K., Jamalli, A., Zig, L., & Putzer, H. (2009). RNase Y, a novel endoribonuclease, initiates riboswitch turnover in Bacillus subtilis. *The EMBO Journal*, *28*(22), 3523–3533. https://doi.org/10.1038/EMBOJ.2009.283

Sharma, C. M., Hoffmann, S., Darfeuille, F., Reignier, J., Findeiß, S., Sittka, A., Chabas, S., Reiche, K., Hackermüller, J., Reinhardt, R., Stadler, P. F., & Vogel, J. (2010). The primary transcriptome of the major human pathogen Helicobacter pylori. *Nature*, *464*(7286), 250–255. https://doi.org/10.1038/NATURE08756

Smirnov, A., Förstner, K. U., Holmqvist, E., Otto, A., Günster, R., Becher, D., Reinhardt, R., & Vogel, J. (2016). Grad-seq guides the discovery of ProQ as a major small RNA-binding

protein. *Proceedings of the National Academy of Sciences of the United States of America*, *113*(41), 11591–11596. https://doi.org/10.1073/PNAS.1609981113

Suzuki, S., Esaki, M., Kusano, C., Ikehara, H., & Gotoda, T. (2019). Development of Helicobacter pylori treatment: How do we manage antimicrobial resistance? *World Journal of Gastroenterology*, *25*(16), 1907–1912. https://doi.org/10.3748/WJG.V25.I16.1907

Svensson, S. L., & Sharma, C. M. (2021). RNase III-mediated processing of a trans-acting bacterial sRNA and its cis-encoded antagonist. *ELife*, *10*. https://doi.org/10.7554/ELIFE.69064

Tejada-Arranz, A., & de Reuse, H. (2021). Riboregulation in the Major Gastric Pathogen Helicobacter pylori. *Frontiers in Microbiology*, *12*. https://doi.org/10.3389/FMICB.2021.712804

Tejada-Arranz, A., de Crécy-Lagard, V., & de Reuse, H. (2020). Bacterial RNA Degradosomes: Molecular Machines under Tight Control. *Trends in Biochemical Sciences*, *45*(1), 42–57. https://doi.org/10.1016/J.TIBS.2019.10.002

Tejada-Arranz, A., Galtier, E., el Mortaji, L., Turlin, E., Ershov, D., & de Reuse, H. (2020). The RNase J-Based RNA Degradosome Is Compartmentalized in the Gastric Pathogen Helicobacter pylori. *MBio*, *11*(5). https://doi.org/10.1128/MBIO.01173-20

Thomason, M. K., & Storz, G. (2010). Bacterial antisense RNAs: how many are there, and what are they doing? *Annual Review of Genetics*, *44*, 167–188. https://doi.org/10.1146/ANNUREV-GENET-102209-163523

Tomb, J. F., White, O., Kerlavage, A. R., Clayton, R. A., Sutton, G. G., Fleischmann, R. D., Ketchum, K. A., Klenk, H. P., Gill, S., Dougherty, B. A., Nelson, K., Quackenbush, J., Zhou, L., Kirkness, E. F., Peterson, S., Loftus, B., Richardson, D., Dodson, R., Khalak, H. G., … Craig Venter, J. (1997). The complete genome sequence of the gastric pathogen Helicobacter pylori. *Nature*, *388*(6642), 539–547. https://doi.org/10.1038/41483

Vannini, A., Agriesti, F., Mosca, F., Roncarati, D., Scarlato, V., & Danielli, A. (2012). A convenient and robust in vivo reporter system to monitor gene expression in the human pathogen Helicobacter pylori. *Applied and Environmental Microbiology*, *78*(18), 6524–6533. https://doi.org/10.1128/AEM.01252-12

Vannini, A., Pinatel, E., Costantini, P. E., Pelliciari, S., Roncarati, D., Puccio, S., de Bellis, G., Peano, C., & Danielli, A. (2017). Comprehensive mapping of the Helicobacter pylori NikR regulon provides new insights in bacterial nickel responses. *Scientific Reports*, *7*. https://doi.org/10.1038/SREP45458

Vannini, A., Roncarati, D., & Danielli, A. (2016). The cag-pathogenicity island encoded CncR1 sRNA oppositely modulates Helicobacter pylori motility and adhesion to host cells. *Cellular and Molecular Life Sciences : CMLS*, *73*(16), 3151–3168. https://doi.org/10.1007/S00018-016-2151-Z

Vannini, A., Roncarati, D., D'Agostino, F., Antoniciello, F., & Scarlato, V. (2022). Insights into the Orchestration of Gene Transcription Regulators in Helicobacter pylori. *International Journal of Molecular Sciences*, *23*(22), 13688. https://doi.org/10.3390/IJMS232213688

Vannini, A., Roncarati, D., Spinsanti, M., Scarlato, V., & Danielli, A. (2014). In depth analysis of the Helicobacter pylori cag pathogenicity island transcriptional responses. *PloS One*, *9*(6). https://doi.org/10.1371/JOURNAL.PONE.0098416

Varadi, M., Anyango, S., Deshpande, M., Nair, S., Natassia, C., Yordanova, G., Yuan, D., Stroe, O., Wood, G., Laydon, A., Zídek, A., Green, T., Tunyasuvunakool, K., Petersen, S., Jumper, J., Clancy, E., Green, R., Vora, A., Lutfi, M., … Velankar, S. (2022). AlphaFold Protein Structure Database: massively expanding the structural coverage of protein-sequence space with high-accuracy models. *Nucleic Acids Research*, *50*(D1), D439–D444. https://doi.org/10.1093/NAR/GKAB1061

Vogel, J., & Luisi, B. F. (2011). Hfq and its constellation of RNA. *Nature Reviews. Microbiology*, *9*(8), 578–589. https://doi.org/10.1038/NRMICRO2615

Vogelmann, R., & Amieva, M. R. (2007). The role of bacterial pathogens in cancer. *Current Opinion in Microbiology*, *10*(1), 76–81. https://doi.org/10.1016/J.MIB.2006.12.004

Voss, B. J., Gaddy, J. A., McDonald, W. H., & Cover, T. L. (2014). Analysis of surface-exposed outer membrane proteins in Helicobacter pylori. *Journal of Bacteriology*, *196*(13), 2455–2471. https://doi.org/10.1128/JB.01768-14

Waidner, B., Melchers, K., Stähler, F. N., Kist, M., & Bereswill, S. (2005). The Helicobacter pylori CrdRS two-component regulation system (HP1364/HP1365) is required for copper-mediated induction of the copper resistance determinant CrdA. *Journal of Bacteriology*, *187*(13), 4683–4688. https://doi.org/10.1128/JB.187.13.4683-4688.2005

Waite, D. W., Vanwonterghem, I., Rinke, C., Parks, D. H., Zhang, Y., Takai, K., Sievert, S. M., Simon, J., Campbell, B. J., Hanson, T. E., Woyke, T., Klotz, M. G., & Hugenholtz, P. (2017). Comparative Genomic Analysis of the Class Epsilonproteobacteria and Proposed Reclassification to Epsilonbacteraeota (phyl. nov.). *Frontiers in Microbiology*, *8*(APR). https://doi.org/10.3389/FMICB.2017.00682

Wen, Y., Feng, J., & Sachs, G. (2013). Helicobacter pylori 5'ureB-sRNA, a cis-encoded antisense small RNA, negatively regulates ureAB expression by transcription termination. *Journal of Bacteriology*, *195*(3), 444–452. https://doi.org/10.1128/JB.01022-12

Xiang, Z., Censini, S., Bayeli, P. F., Telford, J. L., Figura, N., Rappuoli, R., & Covacci, A. (1995). Analysis of expression of CagA and VacA virulence factors in 43 strains of Helicobacter pylori reveals that clinical isolates can be divided into two major types and that CagA is not necessary for expression of the vacuolating cytotoxin. *Infection and Immunity*, *63*(1), 94–98. https://doi.org/10.1128/IAI.63.1.94-98.1995

Yu, J. H., Hamari, Z., Han, K. H., Seo, J. A., Reyes-Domínguez, Y., & Scazzocchio, C. (2004). Double-joint PCR: a PCR-based molecular tool for gene manipulations in filamentous fungi. *Fungal Genetics and Biology : FG & B*, *41*(11), 973–981. https://doi.org/10.1016/J.FGB.2004.08.001

Zakharova, N., Paster, B. J., Wesley, I., Dewhirst, F. E., Berg, D. E., & Severinov, K. v. (1999). Fused and overlapping rpoB and rpoC genes in Helicobacters, Campylobacters, and related bacteria. *Journal of Bacteriology*, *181*(12), 3857–3859. https://doi.org/10.1128/JB.181.12.3857-3859.1999

Zannoni, A., Pelliciari, S., Musiani, F., Chiappori, F., Roncarati, D., & Scarlato, V. (2021). Definition of the Binding Architecture to a Target Promoter of HP1043, the Essential Master Regulator of Helicobacter pylori. *International Journal of Molecular Sciences*, *22*(15). https://doi.org/10.3390/IJMS22157848